POLITECNICO DI TORINO

Department of Mechanical Engineering

Master's Degree in Automotive Engineering

MASTER THESIS

Calibration and optimization of the electronic control of a SCR after-treatment system for a Common Rail Off-Road Diesel engine

Candidate:

Simone Lombardo

Advisor:

Prof. Dr.-Ing Federico Millo

Company Supervisors:

Ing. Simone Rocchi

Ing. Fabio Siccardi

KOHLER
IN POWER. SINCE 1920.

Academic year 2020 - 2021

CONFIDENTIALITY CLAUSE

The content of the following diploma thesis is confidential information property of KOHLER Power Design and Development Department, Reggio Emilia. Publication and duplication of this diploma thesis – even in extracts – are strictly forbidden without the formal approval of the KOHLER Power Design and Development Department. It is only allowed to make this diploma thesis assessable to the advisor and co-advisor as well as to the board of examiners from Politecnico di Torino. This lock flag is valid until written approval for publication from the writer and jointly the KOHLER Company.

KOHLER
IN POWER. SINCE 1920.

ABSTRACT

Over the past decade Off-Road emissions legislation framework becomes more stringent. For this reason, OEMs decided to change their internal combustion engines, by adopting new technologies able to reduce pollutant emissions.

The core of the work is focused on the calibration of the SCR Closed Loop dosing control strategy. The Closed Loop is done by comparing the desired NH_3 storage with the modelled one. The latter is based upon detailed chemical models inside the Engine Control Unit.

NH_3 storage tests have been carried out on a real test bench with the aim of characterizing the SCR storage capacity as a function of Space Velocity and SCR inlet temperature. SynGas tests results have been taken as a reference.

To better control the SCR ageing also injection adaption and NH_3 slip detection strategies have been calibrated in the ECU.

Finally, results have been validated over type approval cycles and on worst-case maneuvers, refining the calibration when needed.

The activities covered in this thesis were fundamental in order to obtain an engine ready to be homologated according to EU Stage V limits.

LIST OF CONTENTS

LIST OF FIGURES

LIST OF TABLES

LIST OF SYMBOLS AND ABBREVIATIONS

ICE	Internal Combustion Engine	SO_x	Sulphur Oxides
CI	Compression Ignition	EAS	Exhaust Aftertreatment System
DI	Direct Injection	DOC	Diesel Oxidation Catalyst
TDC	Top Dead Center	DPF	Diesel Particulate Filter
BDC	Bottom Dead Center	SCR	Selective Catalytic Reduction
SOI	Start of Injection	ASC	Ammonia Slip Catalyst
SOC	Start of Combustion	CRT	Continuously Regenerating Trap
EOI	End of injection	SV	Space Velocity
HRR	Heat Release Rate	DEF	Diesel Exhaust Fluid
TCR	Turbo Common Rail	AdBlue	DEF commercial name
CAC	Charge Air Cooler	TWC	Three Ways Catalyst
MAF	Mass Air Flow meter	EU	European Union
EGR	Exhaust Gas Recirculation	EPA	Environmental Protection Agency
ECU	Electronic Control Unit	NRTC	Non-Road Transient Cycle
DCU	Dosing Control Unit	RMC	Ramped Mode Cycle
MPU	Micro Processing Unit	NTE	Not-To-Exceed
ETK	Experimental Target Communication	EMS	Exhaust Measurement System
CAN	Controller Area Network	φ	Fuel-Air equivalence ratio
HC	Unburned Hydrocarbons	α	NH_3/NO_x ratio
CO	Carbon Monoxide	θ_{target}	Closed Loop Target Storage
PM	Particulate Matter	θ_{model}	Modelled Storage
PN	Particulate Number	η_{NOx}	NO_x conversion efficiency
SOF	Soluble Organic Fraction	G_{NH3_store}	NH_3 mass flow [g/s]
NO	Nitric Oxide	G_{exh}	Exhaust mass flow [kg/h]
NO_2	Nitrogen Dioxide	μ_{NH3}	NH_3 molar mass [g/mol]
NH_3	Ammonia	μ_{exh}	Exhaust molar mass [g/mol]
N_2O	Nitrous oxide	R_1	Reaction rate

1. Introduction

1.1. Off-Road diesel engines

Compression Ignition (CI) internal combustion engines (ICEs) are well known in Off-Road applications thanks to their high specific torque. The field in which they operate requires very high reliability because, most of the time, engines operate under high power and load conditions, dust, dirt and vibrations. The low specific power, obtained by adopting large displacements, guarantees low mechanical stress of the main engine's components and hence high reliability.

1.1.1. Diesel Combustion process

In the following, a brief explanation of the diesel engine cycle and the combustion process are made [1]. As it is known, the ICE 4-stroke cycle is made by:

- o **Intake stroke:** the piston moves from TDC to BDC with the intake valves open and draws fresh mixture into the cylinder.
- o **Compression stroke:** all the valves are closed and the air inside the cylinder is compressed by the piston motion from BDC to TDC.
- o **Expansion stroke:** combustion process occurs between the end of the compression stroke and the first part of the expansion stroke. The energy released by the burning fuel is transferred as pressure energy to the piston. This stroke is also called "Power Stroke".
- o **Exhaust stroke:** the exhaust valves open and the exhaust gas is discharged into atmosphere because the working fluid needs to be replaced by a fresh mixture.

In Figure 1.1.1, an ideal diesel engine cycle is shown:
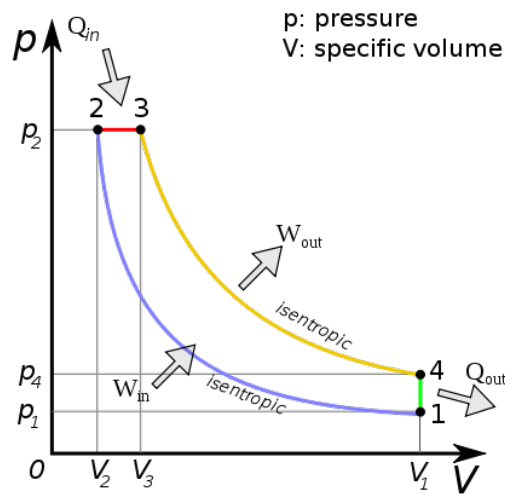
Figure 1.1.1 - p-V diagram of an ideal Diesel cycle

In Direct Injection CI engines, the fuel is injected by the fuel-injection system directly inside the combustion chamber at the end of the compression stroke, just before the desired start of combustion (SOC). The fuel is injected by several nozzles in the injector tip that atomize the liquid phase into several droplets, as shown in Figure 1.1.2. These small droplets, entering in contact with high pressure and temperature ambient, vaporize and mix with the surrounding air.
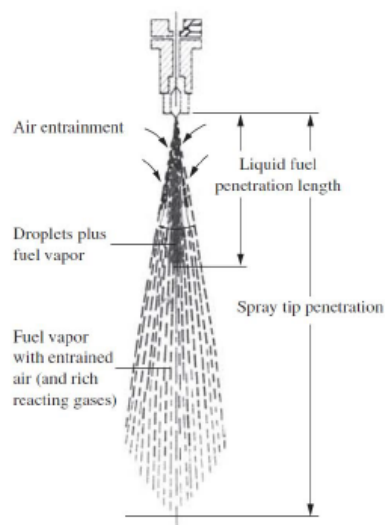
Figure 1.1.2 - Diesel fuel spray

Once the flammability limit is reached, combustion process starts and continues until the end of the injection. The time needed between the SOI and the SOC is called Ignition Delay. Differently from SI (Spark Ignition) engines that adopt low reactivity fuel mixed with the in-cylinder air during the intake stroke, CI ones use high reactivity fuel that must be injected slightly before the desired SOC. For this reason, knock limits typical of SI engines, are not a problem for CI ones and higher compression ratio can be used thus leading to higher engine efficiency. Since the combustion process occurs within and around the fuel spray, engine torque can be controlled by varying the amount of fuel injected per cycle, with the air flow unchanged [2] [3].

The main stages of CI combustion process are shown in Figure 1.1.3 [4]:
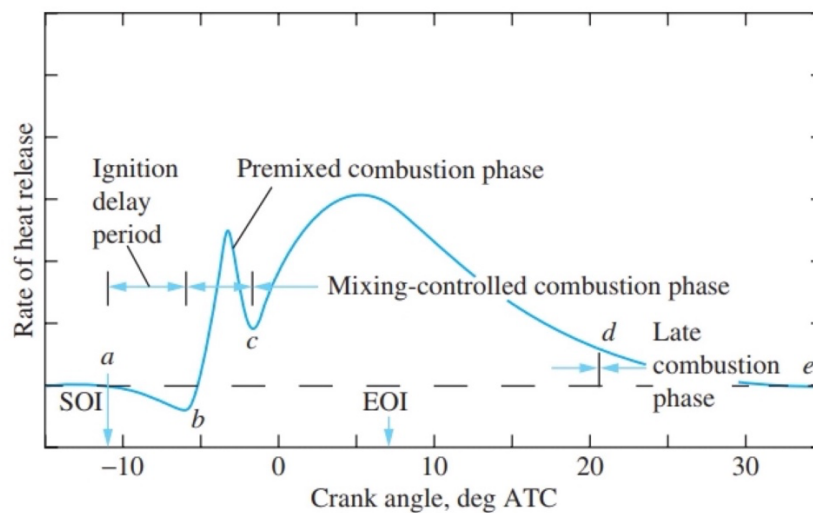
Figure 1.1.3 - Typical Diesel DI engine heat-release-rate diagram

1. Ignition Delay: time interval between SOI and SOC. It is caused by physical (fuel jet atomization, vaporization and mixing) and chemical (preliminary reactions) causes.
2. Premixed combustion phase: almost instantaneously burning of the fuel cumulated inside the combustion chamber during the ignition delay.
3. Mixing-controlled burning phase: the burning rate or the HRR is controlled by the rate at which new mixture becomes available.
4. Late combustion phase.

1.1.2. The KDI engine family

The KDI engine family includes 3- and 4-cylinders engines with a displacement range between 1.9L and 3.4L. They are divided into mechanical and electronic ones. The mechanical engines are fed by a mechanical pump with a radial distributor that split the high-pressure fuel between injectors. Instead, the electronic ones adopt a common rail system made of a high-pressure pump and several electronically controlled injectors. The common rail solution, shown in Figure 1.1.4, ensures the capability to perform multiple injections strategies and it guarantees a better fuel atomization due to the higher injection pressure.
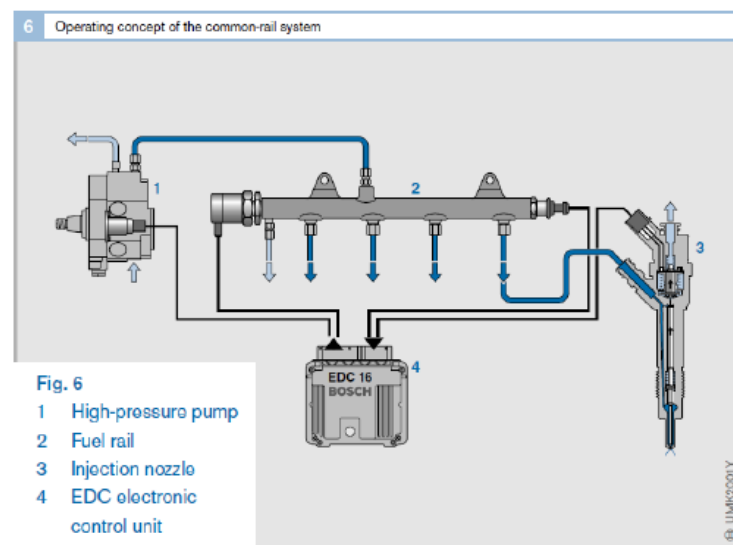
Figure 1.1.4 - Schematic concept of the common-rail system

Figure 1.1.5 shows the KDI 3404 Stage V, which is the subject of this thesis.

Figure 1.1.5 - KDI 3404 TCR Stage V with engine mounted ATS

The main features of the KDI 3404 Stage V are reported in Table 1.1.1 :

Number of cylinders	4
Rated Power	105 kW (2200 rpm)
Maximum Torque	650 Nm (1400 rpm)
Number of valves per cylinder	4
Displacement	3359 cm^3
Bore	96 mm
Stroke	116 mm
Injection system	Common Rail (2000 bar)
Injector type	Solenoidal
Aftertreatment System	DOC+DPF+SCR+ASC

Table 1.1.1 - Engine features

The rated power in Table 1.1.1 is called "parent" calibration, which is the setting with the highest amount of fuel introduction. During certification test this calibration is the only one which is tested but it is possible to sell the engine also with different rated power for customer which requires so.

Further features:

- o A turbocharger with CAC (Charge Air Cooler) is adopted to increase the air mass entering inside the cylinder by cooling down the compressed air. The maximum boost pressure is controlled by a wastegate.
- o The MAF (Mass Air Flow Meter) is replaced by an air mass model calculated by ECU and based on intake pressure, temperature and EGR mass flow.
- o The EGR valve is not present. This solution leads to a more reliable and cheaper engine, but it requires a well-designed and well-calibrated SCR control system.
- o A throttle valve is adopted to increase the exhaust gas temperature under part load operating conditions for thermal management of EAS and DPF regeneration.

1.2. Electronic Control Unit (ECU)

The application of ECUs (Figure 1.2.1) to Internal Combustion Engines allow to better control the combustion process by a more precise injection metering and timing. The electronic control of the main engine actuators led to both a reduction of engine out emissions and the possibility to modify the combustion mode according to the aftertreatment needs (e.g.: Normal mode, SCR Heat-Up, DOC Heat-Up, Regeneration).
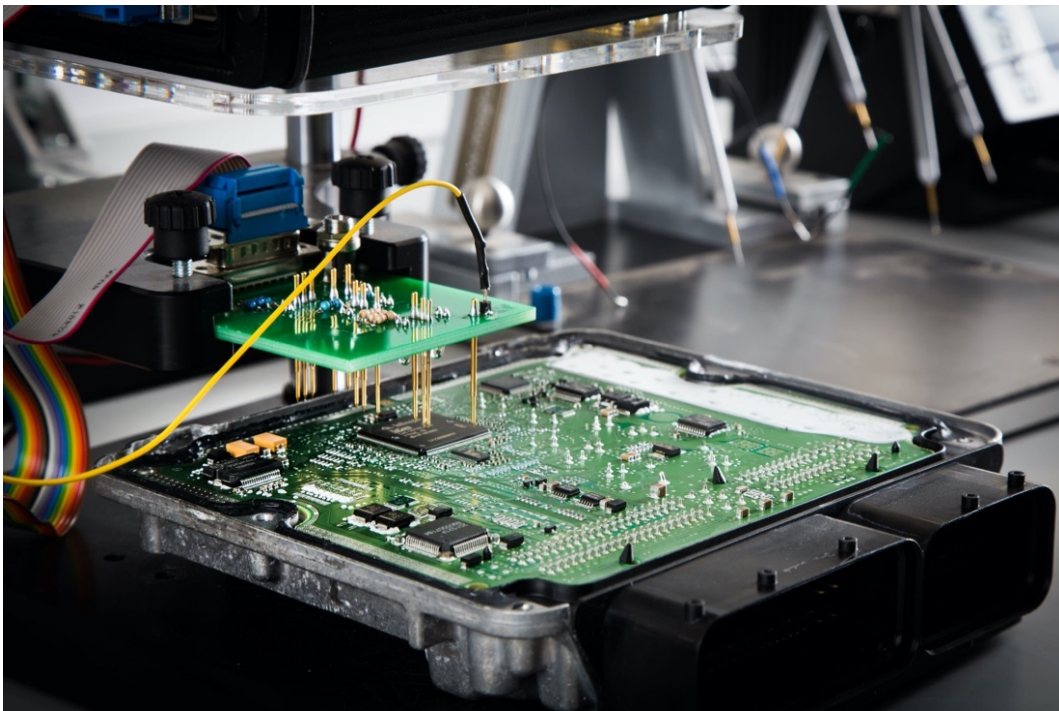
Figure 1.2.1 - Electronic Control Unit

ECUs can be divided into three main groups [5]:

o   Open ECUs with ETK communication protocol: they are used during the calibration development process because they allow online calibration without having to switch-off the engine.

o   Open ECUs with CCP (CAN calibration protocol) communication protocol: They are adopted for minor development activity such as endurance and durability tests. Using this hardware, online calibration is not allowed, and the dataset can be changed only with the engine switched off.

o   Closed ECUs: They are those ECUs with which the production engines are equipped. They don't allow any calibration activity.

1.2.1. Hardware

ECU – Simplified layout
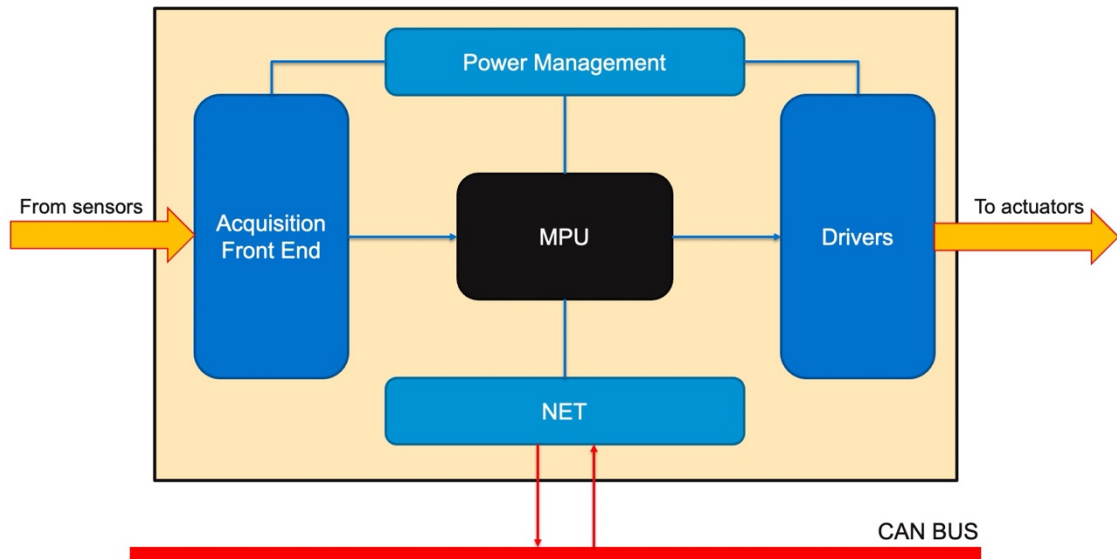
Figure 1.2.2 - Simplified layout of an ECU

The hardware core is represented by the MPU (Micro Processing Unit). It is involved in processing data coming from the acquisition front end (sensors) and the CAN BUS (driver requests and other ECUs outputs). It can both act by means of drivers on actuators and communicate its outputs to other ECUs connected to the CAN BUS.

1.2.2. Software

On ECU's data memory, a software is installed. The action of replacing the software version on an ECU is known as "flashing". The software used in Kohler company has a format **.s19** and it is written in hexadecimal system. In general any software is paired with a description file (format **.a2l**) which associates a collocation, a label, a description for each string of data [6].
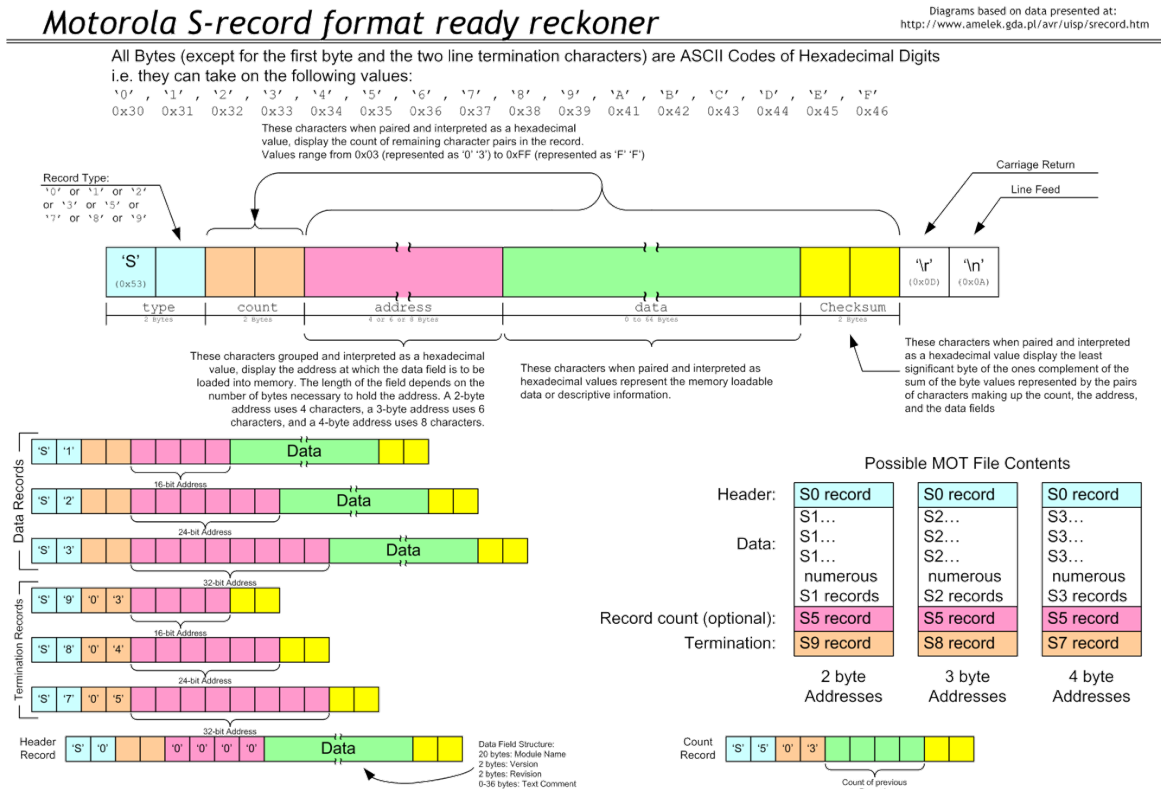
Figure 1.2.3 - Motorola S-record format ready reckoner (.s19)

Any **.s19** file is formed by a series of 24-bytes strings, as shown in Figure 1.2.3. Each of them can be divided into:

- o **1 byte** of heading
- o **1 byte** of count
- o **4 bytes** of address (defining the destination of the carried data)
- o **16 bytes** of data (descriptive information)
- o **1 byte** of checksum of count, address and data fields
- o **1 byte** of carriage return
- o **1 byte** of line feed.

Software can be divided in two main parts:

- o **Code:** it contains the logic that the processor must follow in evaluating the instantaneous value of variables. It is written in programming language by a company supplier.

- o **Dataset:** it includes reference data and calibration variables. In an open ECU, it can be further divided into a part containing the base values of every dataset variable (called Reference Page in ETAS Inca interface tool) and a second one showing the actual customizable values (Working Page). The WP is used by calibration engineers to modify ECU parameters in real time.

1.3. Primary Pollutants Formation and Control

Reaction (1.1) represents the ideal combustion process:

$$C_aH_b + \left(a + \frac{b}{4}\right)(O_2 + 3.773N_2) = aCO_2 + \frac{b}{2}H_2O + 3.773\left(a + \frac{b}{4}\right)N_2 \qquad (1.1)$$
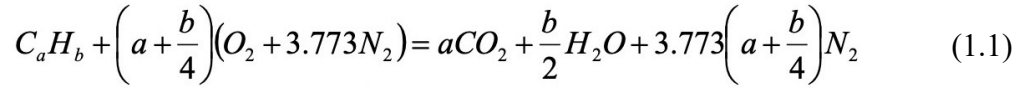
Although ideal combustion reaction of hydrocarbon fuels should lead to non-toxic combustion products, the real combustion process produces pollutant emissions (mainly represented by HC, CO, PM, NO_x) [4].
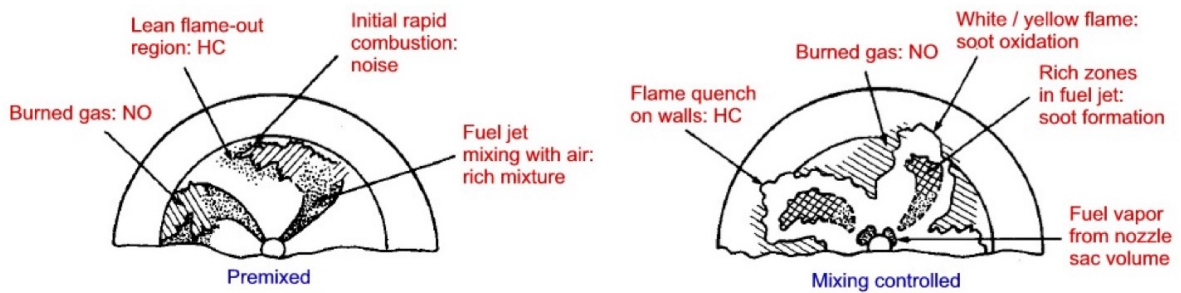
Figure 1.3.1 - Summary of pollutant formation mechanisms in a Direct-Injection Diesel engine

Although CI engines always work with an overall lean mixture, the fuel distribution inside the combustion chamber is highly non uniform. The pollutant formation processes are strongly dependent on the fuel distribution and how that distribution changes with time due to mixing with the in-cylinder air [3]. Figure 1.3.1 shows how various regions of the fuel spray and diffusion flame affect the formation of NO, HC and Soot during the "premixed" and "mixing controlled" phases of diesel combustion in a DI engine with swirl.

1.3.1. Hydrocarbons and Carbon Monoxide

Diesel engines are not a significant source of Carbon Monoxide (CO) because they operate with an overall lean equivalence ratio ($\varphi < 0.9$) [3].

HC emissions of a diesel engine vary over a large molecular size range because diesel fuel contains hydrocarbon compounds with high molecular weight. There are several processes that could contribute to diesel hydrocarbon emissions, Figure 1.3.2 illustrates how these processes can produce incomplete combustion products [3].
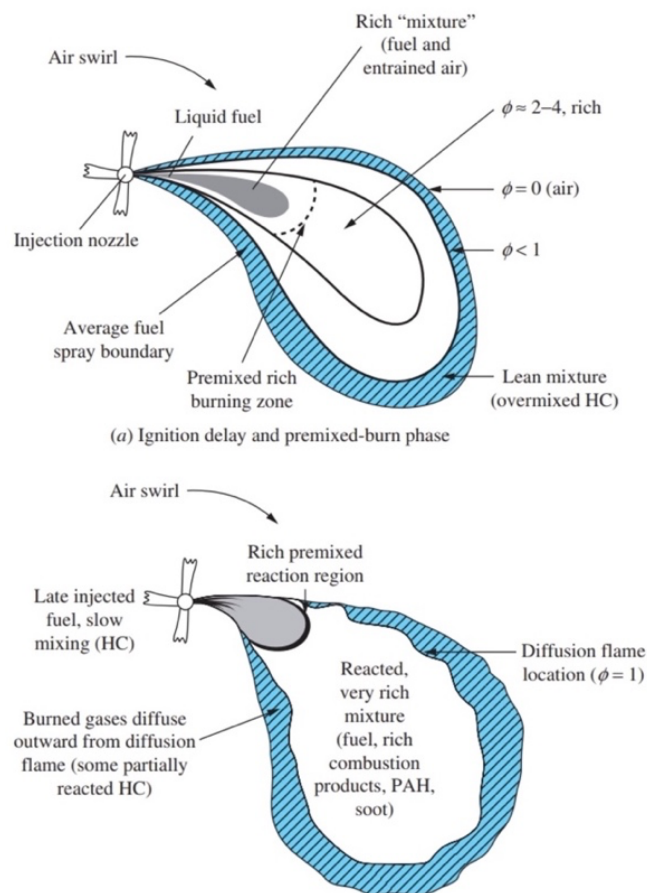
Figure 1.3.2 - Schematic representation of the diesel HC formation mechanism

1. Overleaning:

During the ignition delay, the amount of fuel that is mixed leaner than the lean combustion limit increases with time. This mixture can only oxidize by relatively slow oxidation reactions which may not be complete. The magnitude of unburned hydrocarbons due to these

overlean regions depend on the amount of fuel injected during the ignition delay and the mixing process with in-cylinder air during this time.

2. Undermixing

The two sources of fuel under mixing with in-cylinder air are:

- o Fuel remaining inside the injector sac volume at the EOI. As the combustion and expansion processes proceed, this fuel is heated, vaporizes and enters in the cylinder at low velocity. Hence, the fuel vapour will mix slowly with the surrounding air and may escape the primary combustion process.
- o Excess of fuel that enters in the cylinder under overfueling conditions (smoke limit). Under acceleration transient conditions, overfueling can occur. Although the overall equivalence ratio remains lean, locally over-rich conditions may persist through the expansion stroke and into the exhaust process.

3. Quenching and Misfire

Wall quenching of the flame may also be a significant source of HC emissions, depending on the degree of spray impingement on the combustion chamber walls.

1.3.2. Particulate Matter

Particulate Matter is defined as any matter in the exhaust gas flow of an internal combustion engine that can be trapped on a sampling filter medium at 52°C [4]. Figure 1.3.3 illustrates the typical PM composition:
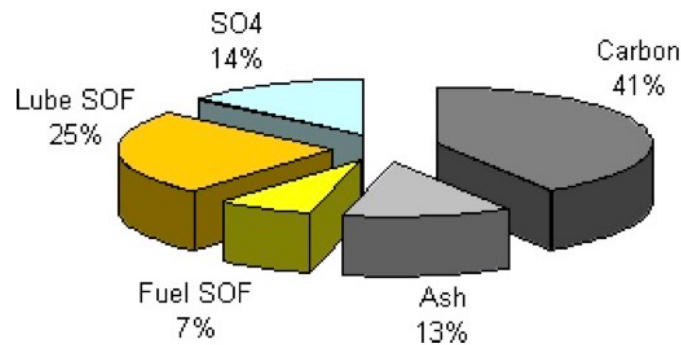
Figure 1.3.3 – Typical Particulate Matter composition

- o Soluble Organic Fraction (**SOF**) can be derived from both lubricant and fuel.
- o **ASHES** mainly derive from lubricant oil and fuel additives. Their presence compromises the functioning of the DPF aftertreatment system (1.3.4) because they don't burn during regeneration.
- o **SO$_4$** depend on lubricant oil and fuel sulphur content.
- o **Soot** is formed during a real combustion process when fuel burns extremely rich (φ > 4) under relatively low temperature (T < 1600K). Soot formed during the premixed burning phase (φ > 4) is largely oxidized while the combustion process develops. Tail pipe soot emissions are mainly related to fuel remaining into the injector sac because it enters slowly inside the combustion chamber and burns under rich and low temperature conditions [4].

1.3.3. Nitrogen Oxides

NO_x emissions of Diesel engines are usually 70-90% NO and 30-10% NO_2. NO forms as a by-product of the combustion process and then NO_2 forms from NO.

The main formation mechanism is the thermal one, also called **extended Zeldovich mechanism** [3]. The three reactions governing this mechanism are:

$$O + N_2 \rightarrow NO + N \tag{1.2}$$

$$N + O_2 \rightarrow NO + O \tag{1.3}$$

$$N + OH \rightarrow NO + H \tag{1.4}$$

Reaction (1.1) has a high activation energy, resulting in a high sensitivity to temperature. The mechanism becomes relevant at high temperature (T > 2000K) and at air-fuel mixture that are close to stochiometric (diffusion flame zone). The temperature sensitivity of this mechanism also means that as the temperature in the combustion chamber drops during the expansion stroke, the NO concentration freezes. NO formed in the flame zone can be rapidly converted into NO_2 via reaction (1.5).

$$NO + HO_2 \rightarrow NO_2 + OH \tag{1.5}$$

$$NO_2 + O \rightarrow NO + O_2 \tag{1.6}$$

Conversion of NO_2 to NO occurs via reaction (1.6) unless the NO_2 so formed is quenched by mixing with the surrounding cooler air. This explanation is consistent with the biggest NO_2/NO ratio occurring at light load in diesel engines. NO_2 production is important for some aftertreatment systems, such as DPF (CRT effect) and SCR [4].

1.3.4. Exhaust Aftertreatment System

In addition to in-cylinder techniques to reduce pollutants (e.g.: injection pressure, multiple injections, injection timing, EGR recirculation, etc...), exhaust aftertreatment systems are required to meet the more stringent emission regulations. While the former are not the subject of this discussion, the latter are described with particular interest in SCR system.

CI engines burn an overall lean air-fuel mixture thus leading to an exhaust environment with high oxygen concentration. Hence, a TWC cannot be adopted even if it is the best technology available to reduce the three main primary pollutants (HC, CO, NO_x) [3].

There are several aftertreatment layouts in worldwide applications. The layout shown in Figure 1.3.4 is the one adopted in the KDI 3404 TCR Stage V and generally in Off-Road applications with a rated power above 56 kW to meet current emission legislation.

Figure 1.3.4 - Exhaust Aftertreatment System scheme of the KDI 3404 TCR Stage V

The EAS of the KDI 3404 TCR Stage V is made by:

- o **DOC**: "Flow Through" aftertreatment system able to control HC and CO emissions with high efficiency. Catalytic oxidation is promoted by precious metals, generally by means of Platinum on an alumina washcoat [4]. The DOC hydrocarbons activity extends to compounds such as SOF, thus partially reducing diesel PM emission. However, DOC also promotes sulphur oxidation (unwanted effect) and NO oxidation into NO_2 (important to improve CRT effect in the DPF and NO_x conversion efficiency in the SCR) [4].

o **DPF:** "Wall Through" aftertreatment system capable of removing PM from the exhaust by means of mechanical filtration. DPF needs to be regenerated periodically in order to burn the soot accumulated inside the trap. Temperature above 600°C are needed during regeneration, these temperature levels may hardly be reached in the exhaust gas stream of a diesel engine, especially at part load conditions, thus requiring the adoption of specific software strategies to increase the exhaust temperature. Often these strategies lead to fuel consumption penalty, thus a trade-off between fuel penalty due to the pressure drop across the DPF and the one caused by these strategies has to be found [4].

o **Mixer:** it is used to mix the reducing agent (AdBlue), injected though an injector, with the exhaust gas flow, so as to obtain a better distribution and to avoid Urea crystallization.

o **SCR:** it represents one of the possible solutions to reduce NO_x emissions in a plenty of oxygen environment. It ensures a good conversion efficiency without affecting fuel consumption, by using Urea as reducing agent that must be refuelled periodically. Its working principle is described in Chapter 2.1.

o **ASC:** it provides a selective ammonia (NH_3) oxidation function. It is usually adopted when an aftertreatment system is equipped with an SCR catalyst because a significant amount of NH_3 could leave the SCR during dynamic engine cycles and being NH_3 an emission regulated gas.

1.4. Emission regulations

1.4.1. Type approval Test Cycles

Testing sequence:

1. NRTC (preconditioning), the number of preconditioning cycles is chosen by Kohler and declared to the type-approval specialists.

2. One-day soak.

3. NRTC complete procedure (one cold cycle, followed by a 20 minutes of soak time, then one hot cycle).

4. Engine heat-up at a fixed point (50% of max speed, 50% of maximum torque at this speed).

5. RMC.

6. NTE (3 random points chosen by the type-approval specialist).

Non-Road Transient Cycle (NRTC)

The NRTC is a type approval cycle for mobile off-road diesel engines developed by US EPA in cooperation with European Union authorities. The cycle is an engine dynamometer transient driving schedule of total duration of 1238 seconds, exploiting the total range of torque and speed as shown in Figure 1.4.1 and which traces are illustrated in Figure 1.4.2.
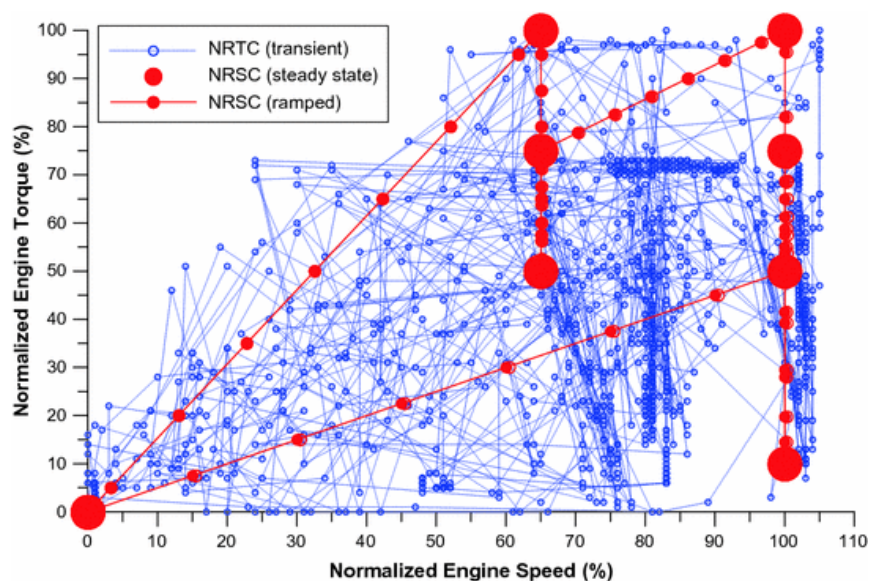
Figure 1.4.1 - Engine working points on NRTC and RMC
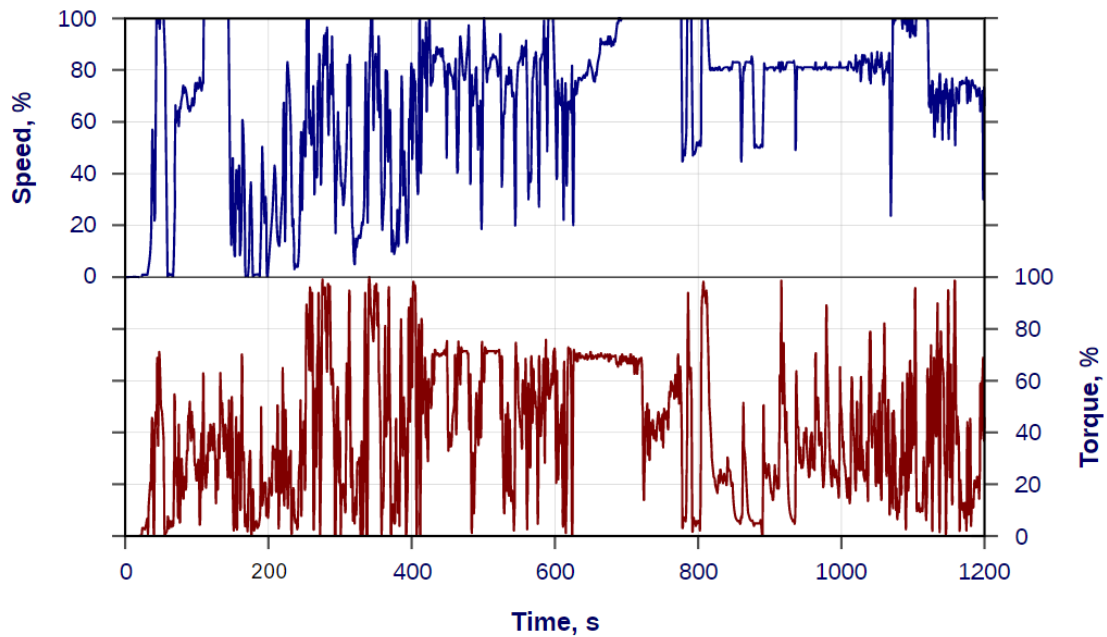
Figure 1.4.2 - Non-Road Transient Cycle

The NRTC represents the engine working conditions while mounted on different vehicles:

- o Backhoe loader
- o Rubber-tire loader
- o Crawler dozer
- o Tractor
- o Excavator
- o Arc welder
- o Skid steer loader

The cycle is run twice, with a cold and a hot start. The cold cycle is run when coolant and lubricant oil are at ambient temperature and the hot one after a soak time of 20 minutes. The emission results of the two parts are considered in EU as a weighted average, counting 10% for the cold run and 90% for the hot one [7].

Ramped Mode Cycle (RMC)

According to ISO 8178 international standards, the engine under investigation must be tested on an engine dynamometer over a sequence of 8 steady-state modes. The engine must be operated for the prescribed time in each mode. The specified speed shall be held to within ±50 rpm and the specified torque shall be held to within ±2% of the maximum torque at the test speed. Differently from the previous Discrete Mode Cycle, the Ramped Mode one is performed as a continuous cycle with standardized ramped transitions between the individual modes, illustrated through red lines and red dots in Figure 1.4.1. Emissions are measured over the whole cycle and each mode contribution is weighted based on the time spent in that mode; Figure 1.4.3 shows the trace of the cycle. The final emission results are expressed in g/kWh [7].
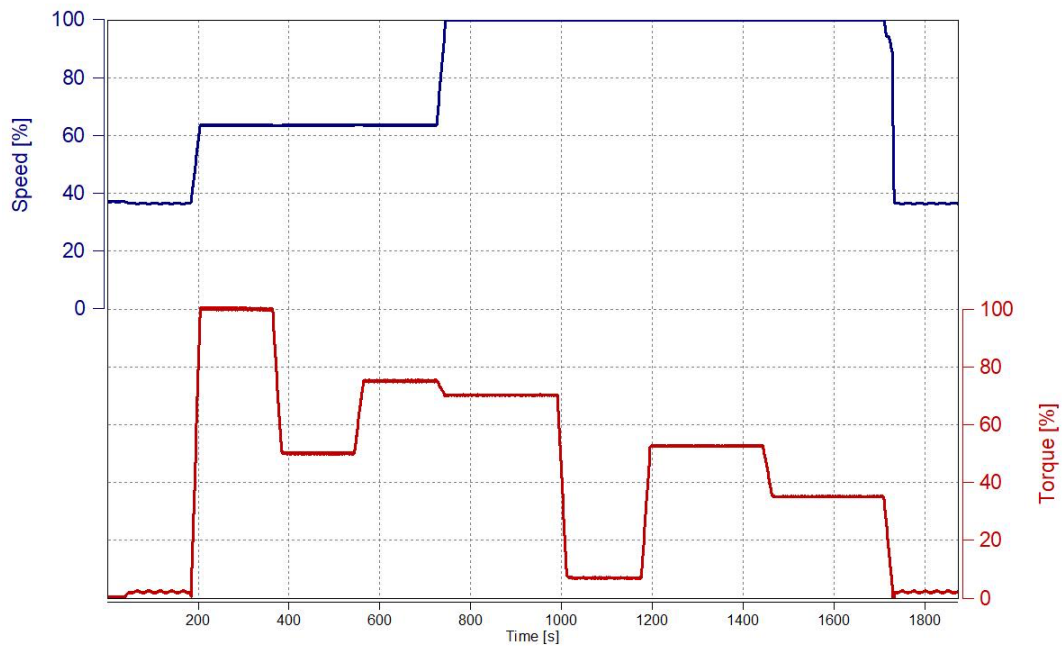
Figure 1.4.3 - Ramped Mode Cycle

Not-To-Exceed (NTE)

The US EPA has introduced not-to-exceed (NTE) emission limits and testing requirements as an additional instrument to make sure that heavy-duty engine emissions are controlled over the full range of speed and load combinations commonly experienced in real use. Three random engine working points are chosen by the type-approval specialist within the NTE Control Area bounds (highlighted area in Figure 1.4.4). Emissions are averaged over a minimum time of thirty seconds and then compared to the applicable NTE emission limits [7].
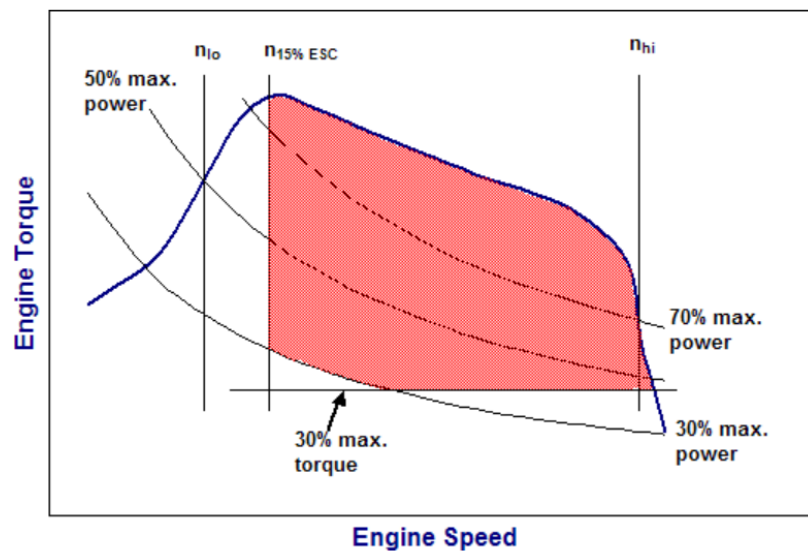
Figure 1.4.4 - Not-To-Exceed control area

The NTE Control Area consists of the following engine speed and load points:

1. All engine speeds above:

   $n_{lo} + 0.15 \times (n_{hi} - n_{lo})$

   where:

   o n_{hi} = the highest engine speed on the power curve where 70% of the maximum engine power is still achievable

- o n_{lo} = the lowest engine speed on the power curve where 50% of the maximum engine power is still achievable.

2. All engine load points greater than or equal to 30% or more of the maximum torque value produced by the engine.

3. All speed and load points where the power produced by the engine is less than 30% of the maximum power produced by the engine are excluded.

1.4.2. EU Stage V limits

The regulation was proposed in 2014 and finalized on September 14, 2016. Standards were effective from 2019 for engines below 56 kW and above 130 kW, and from 2020 for engines of 56-130 kW [7].

Category	Ign.	Net Power kW	Date	CO	HC	NOx	PM	PN 1/kWh
				g/kWh				
NRE-v/c-1	CI	P < 8	2019	8.00	7.50[a,c]		0.40[b]	-
NRE-v/c-2	CI	8 ≤ P < 19	2019	6.60	7.50[a,c]		0.40	-
NRE-v/c-3	CI	19 ≤ P < 37	2019	5.00	4.70[a,c]		0.015	1×10^{12}
NRE-v/c-4	CI	37 ≤ P < 56	2019	5.00	4.70[a,c]		0.015	1×10^{12}
NRE-v/c-5	All	56 ≤ P < 130	2020	5.00	0.19[c]	0.40	0.015	1×10^{12}
NRE-v/c-6	All	130 ≤ P ≤ 560	2019	3.50	0.19[c]	0.40	0.015	1×10^{12}
NRE-v/c-7	All	P > 560	2019	3.50	0.19[d]	3.50	0.045	-

[a] HC+NOx
[b] 0.60 for hand-startable, air-cooled direct injection engines
[c] A = 1.10 for gas engines
[d] A = 6.00 for gas engines

Figure 1.4.5 - EU Stage V limits

In Figure 1.4.5, EU Stage V emission limits are listed as a function of the engine power level. Further limits on NH_3 emissions are added when an SCR system is adopted. During type approval cycles the NH_3 tailpipe average emission has not to exceed the limit of 10 ppm. All limits are double when referring to NTE test cycle. Stage V limits obliged to adopt DPF to fulfil PN limits and SCR system to be within NO_x limits when engine power is greater than 56 kW.

2. Selective Catalytic Reduction electronic control

2.1. SCR working principle
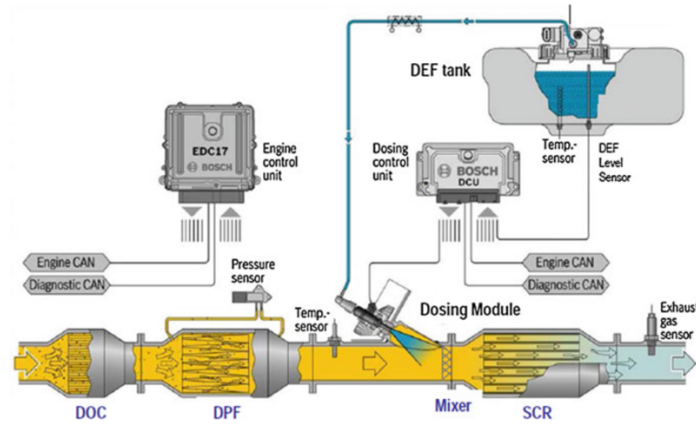
Figure 2.1.1 - Layout of a DOC + DPF + SCR system

The SCR is an aftertreatment system able to reduce NO and NO_2 into N_2 an H_2O by using a water solution with 32% of Urea, called DEF (Diesel Exhaust Fluid) or AdBlue. This solution is injected inside a mixer to get a better mixing with the exhaust gas flow and to avoid crystallization phenomena due to the impact with the exhaust pipe. Urea is thermally decomposed by following the two consecutive reactions [8]:

$$NH_2\text{-}CO\text{-}NH_2 \text{ (Urea)} \rightarrow NH_3 + HNCO \qquad (2.1)$$

$$HNCO + H_2O \rightarrow NH_3 + CO_2 \qquad (2.2)$$
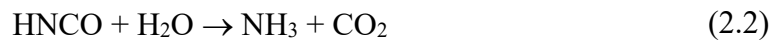
Once ammonia (NH_3) is obtained by thermolysis and hydrolysis reactions, it is absorbed and stored into the substrate of the catalyst where NO_x reduction reactions take place, as shown in Figure 2.1.2:
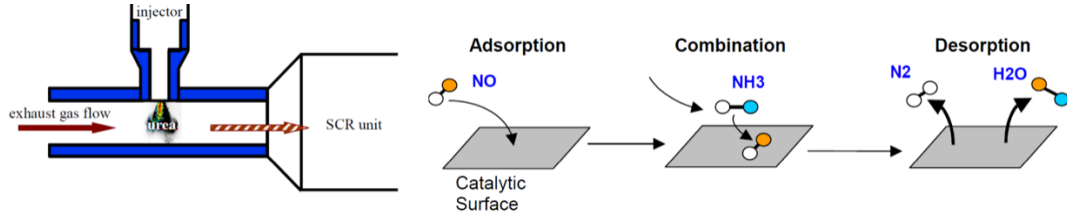
Figure 2.1.2 - Schematic representation of the SCR conversion mechanisms

$$NH_3 + NO + 1/4O_2 \rightarrow N_2 + 3/2\ H_2O \qquad (2.3)$$

$$NH_3 + 1/2NO + 1/2NO_2 \rightarrow N_2 + 3/2\ H_2O \qquad (2.4)$$

$$NH_3 + 3/4NO_2 \rightarrow 7/8N_2 + 3/2\ H_2O \qquad (2.5)$$
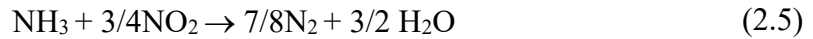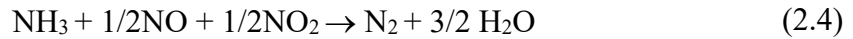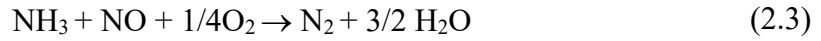
Reaction (2.3) is called "Standard SCR Reaction", it predominates over the other two when the ratio NO_2/NO_x is lower than 0.5. Reaction (2.4) is the fastest and preferred one, but it requires a ratio NO_2/NO_x close to 0.5. Although, the exhaust gas flow of a Diesel engine consists of a greater amount of NO than NO_2, with a ratio strictly dependent on the engine working point, the DOC oxidized part of NO into NO_2 over platinum. The NO_2 so formed promotes the passive regeneration of Soot inside the DPF and brings the ratio NO_2/NO_x closer to 0.5. If the DOC oxidized a too much NO into NO_2, reaction (2.5) becomes relevant and the following side reaction can occur [8]:

$$NH_3 + NO_2 \rightarrow 1/2N_2 + 1/2N_2O + 3/2\ H_2O \qquad (2.6)$$
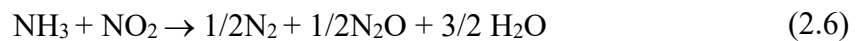
N_2O is a very dangerous greenhouse gas having a warming effectiveness per mole 270 times greater than CO_2. This pollutant emission is not yet regulated but it will certainly be in the future.

If either reactants are not well-mixed or an excess of ammonia is injected to obtain an higher $deNO_x$ efficiency or the NH_3 desorption mechanism is too fast, NH_3 emission can occur. To reduce this, an ASC (Ammonia Slip Catalyst) is adopted [8]:

$$NH_3 + 3/4O_2 \rightarrow 1/2N_2 + 3/2\ H_2O \qquad\qquad (2.7)$$
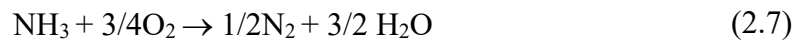
SCR is not a "plug and play" technology. To maximize NO_x conversion efficiency and minimize NH_3 slip, careful total system design and calibration are required [9]. The system can be improved by:

- Optimizing SCR mixer geometry to ensure NH_3 uniformity and to avoid crystallization at low space velocity
- Adopting NO_x sensors upstream and downstream of the SCR catalyst
- Dosing the DEF in Closed Loop
- Optimizing the position of all the aftertreatment systems to guarantee a faster warm-up, since DEF can be injected only when the temperature overcome a certain threshold (180°C-200°C) to avoid crystallization
- Introducing effective EAS warm-up strategies in the ECU software
- Optimizing the DOC precious metal coating to ensure a ratio $NO_2/\ NO_x$ as close as possible to 0.5
- Minimizing the sulphate oxides poisoning effect, calibrating a $deSO_x$ strategy.

While geometry and layout of the SCR system were previously defined, the dosing strategy and its calibration constitute the core of this thesis work.

2.2. Closed Loop control strategy

Rather than an Open Loop dosing control strategy (Figure 2.2.1) based on "α" (ratio between NH_3 and NO_x measured by the sensor upstream the SCR), a Closed Loop one (Figure 2.2.2) was preferred because it allows [10]:

o To maximize NO_x conversion efficiency over the whole temperature operating window and in particular during temperature transient cycles and at low SCR temperature

o To minimize Urea consumption (Customer Satisfaction)

o To minimize NH_3 emissions (Ammonia Slip)
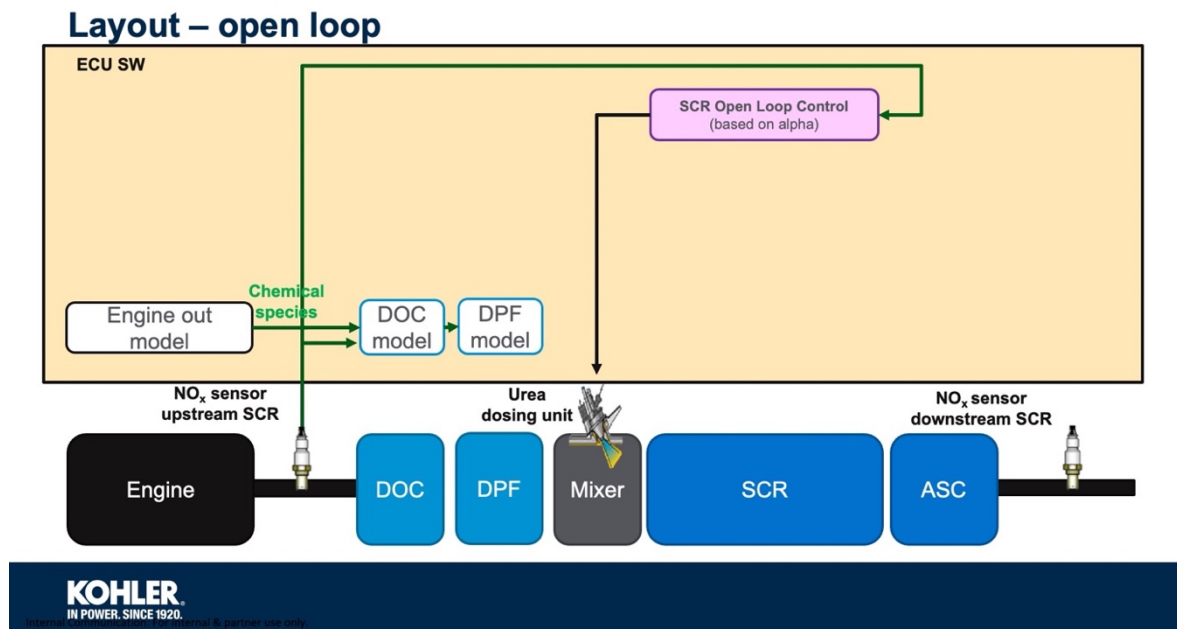
Figure 2.2.1 - Open Loop control strategy layout

The Open Loop control is the simplest dosing strategy, based on the ratio NH_3/NO_x. Two possible alternatives can be considered [10]:

o $NH_3/NO_x < 1 \rightarrow$ Low NO_x conversion efficiency, no risk of emitting NH_3

o $NH_3/NO_x = 1 \rightarrow$ High NO_x conversion efficiency, risk of emitting NH_3 if $NH_3/NO_x > 1$ (e.g.: during fast temperature transients).
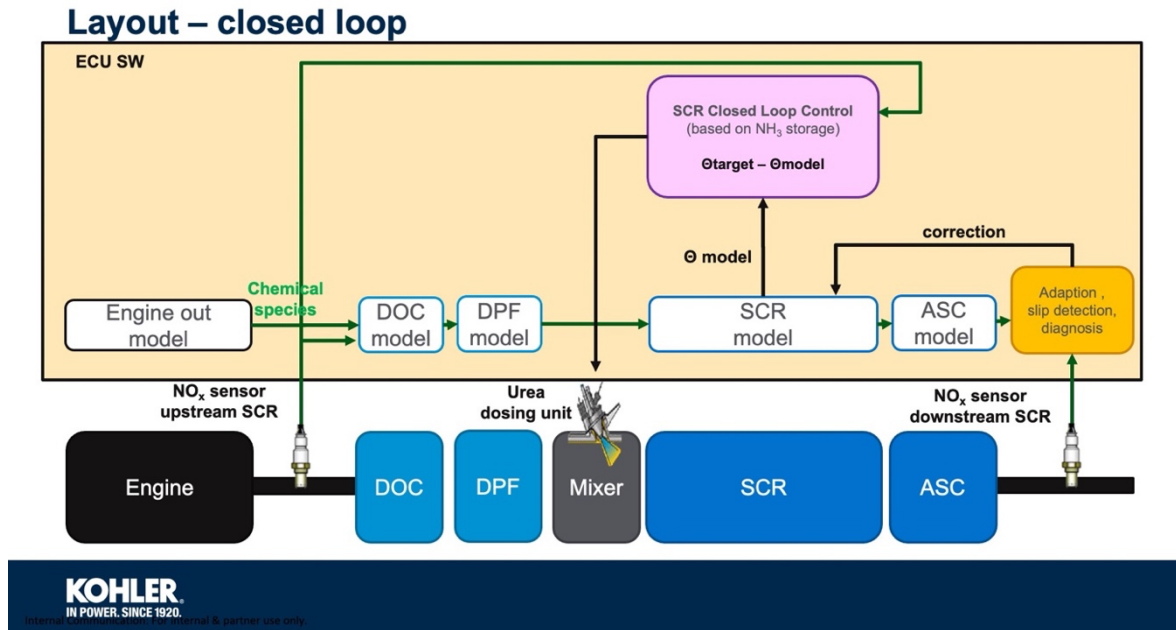
Figure 2.2.2 - Closed Loop control strategy layout

The engine under investigation is controlled by an ECU in which the Closed Loop dosing control strategy in Figure 2.2.2, was decided to be adopted. It is not a simple Closed Loop in which the controller works to minimize the error between target and measured NO_x tailpipe emissions, but it is based on the error between target and modelled NH_3 storage. The NH_3 storage, being a non-measurable quantity, is calculated by a SCR model where most of the chemical reactions are parametrized and calibrated using SynGas tests results. NH_3 storage tests have been carried out on a real test bench to validate the SCR model and to define the NH_3 storage target in order to obtain the desired NO_x conversion efficiency while optimizing ammonia slip during steady state SCR operating conditions and during temperature and space velocity transients.

The Closed Loop controller (schematically shown in Figure 2.2.3) is of the proportional type and can be calibrated to obtain a more or less aggressive pursue of the target. It controls the AdBlue injection quantity in order to reach the desired NH_3 storage (θ_{target}). The closed loop control feedback comes from the storage model (θ_{model}) implemented in the ECU.
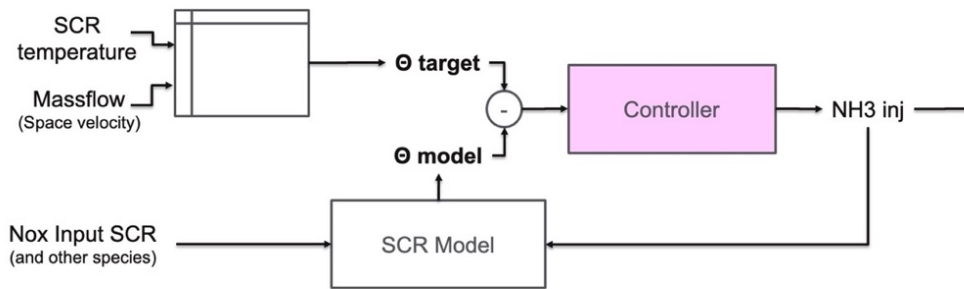
Figure 2.2.3 - Closed Loop controller working principle

2.2.1. Calibration procedure

The following procedure has been followed for the closed loop control calibration:

- o Storage model calibration (already done by a Kohler supplier):
  - Syngas tests
  - Storage and SCR chemical reactions parametrization
- o Storage model validation:
  - NH_3 storage tests on a real test bench at fixed engine operating points
  - Comparison between calculated and modelled storage
- o Storage target definition:
  - To reach the desired NO_x conversion efficiency
  - To avoid NH_3 slip
- o Storage target refinement:
  - SCR temperature steps
  - SCR space velocity steps
- o Closed Loop validation:
  - Emission cycles with aged and fresh EAS
  - Customer cycles with aged and fresh EAS

2.2.2. SCR model (SynGas tests)

Synthesis gas test benches are adopted to characterize the behaviour of the exhaust aftertreatment systems under constant and well-defined working conditions. These tests are needed to parametrize the main chemical reactions and to build physical models able to predict the evolution of the main pollutant species inside the EAS (Figure 2.2.4 shows a schematic representation of the models). Emission models were calibrated with a recursive approach until their results match the real engine ones before being implemented in the ECU.
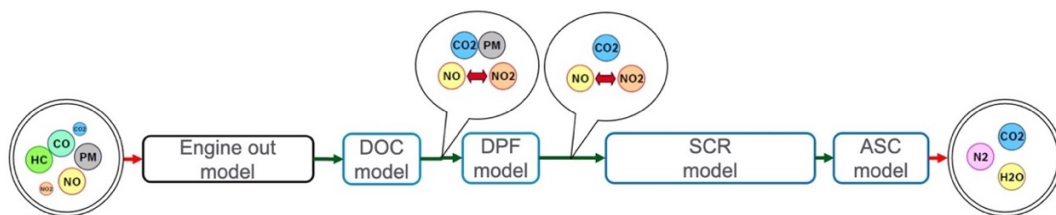
Figure 2.2.4 - Schematic representation of the Exhaust Aftertreatment System models

Sample Preparation

Tests were made on both degreened and aged SCR samples (Figure 2.2.5). They were obtained from full size catalysts. Degreened samples have been treated hydrothermally or in a simulated exhaust atmosphere before installation.
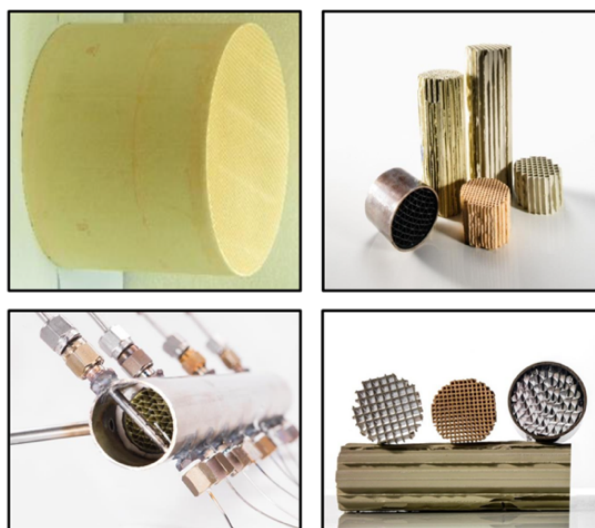
Figure 2.2.5 - SCR degreened and aged samples for SynGas tests

Samples were mounted into pipes equipped with thermocouples, sampling probes and pressure sensors as shown in Figure 2.2.6
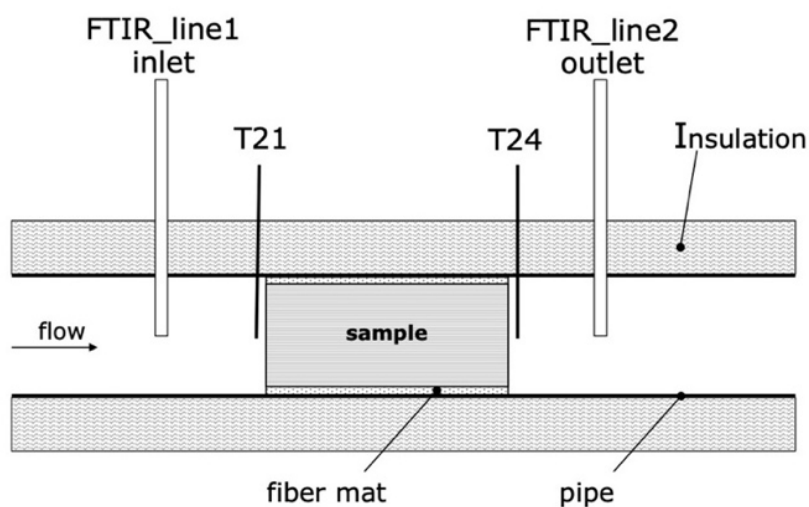
Figure 2.2.6 - SynGas test layout

Experimental setup
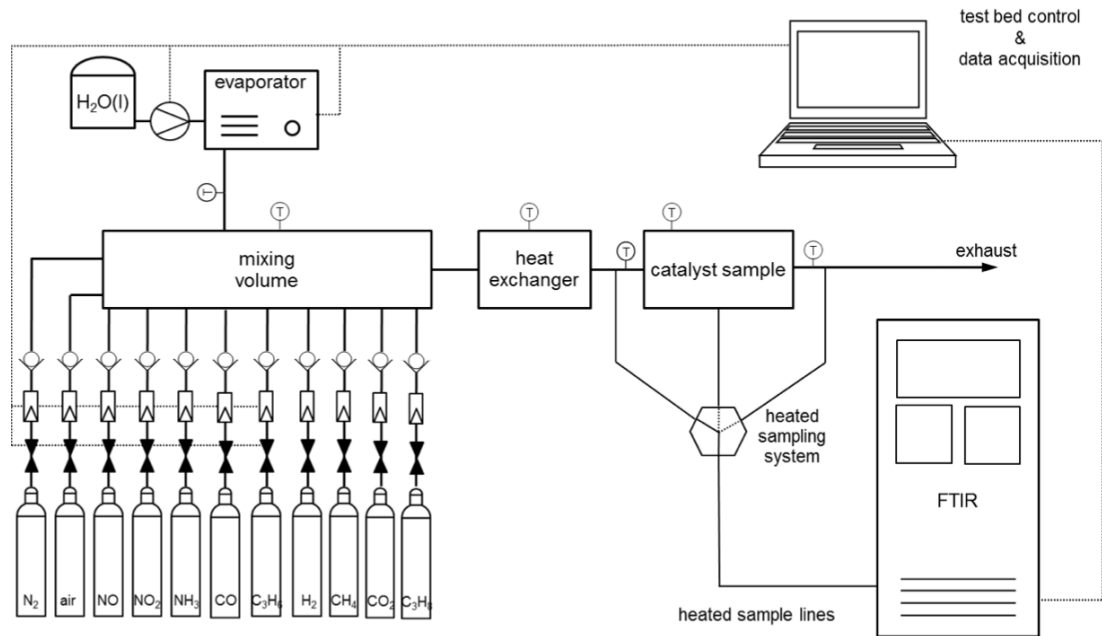
Figure 2.2.7 - SynGas test bench setup

As shown in Figure 2.2.7, samples have been installed in a syngas test bench and sampling probes were connected to a FTIR, a measurement system able to detect and measure the chemical content of the working gas. Purified air has been used as oxygen career and other gas species were provided from gas cylinders. Deionized water has been introduced into the hot gas stream to represent the water content of the exhaust gas. Syngas test benches are able to reproduce steady state conditions with high experimental reproducibility. FTIR lines sample with a rate of 1 Hz both upstream and downstream of the catalyst sample. The gas stream temperature can vary from 100°C to 600°C with an accuracy of +/- 10°C and its composition can be controlled with an accuracy of:

- o +/- 15 ppm for NO, NO_2, NH_3
- o +/- 0.5% for O_2 and H_2O.

Measurement Program

Syngas experiments have been performed with different species compositions in order to parametrize the complete behaviour of the SCR:

- o **NH_3 only:** constant level of NH_3 at different temperatures and space velocities to state the SCR storage capacity and parametrize the absorption and desorption rate
- o **NH_3 and O_2:** NH_3 and O_2 at different temperatures to parametrize NH_3 oxidation as well as the production on NO
- o **NH_3, O_2 and NO:** NO_2/NO_x around 0% to characterize the standard SCR reaction (2.3) and N_2O formation
- o **NH_3, O_2, NO and NO_2:** NO_2/NO_x around 50% to characterize the fast SCR reaction (2.4) and N_2O formation
- o **NH_3, O_2, NO and NO_2:** NO_2/NO_x around 75% to characterize the slow SCR reaction (2.5) and N_2O formation.

SCR syngas results

Tests have been carried out at different space velocities, temperatures and NH_3 concentrations over degreened and aged samples.

Figure 2.2.8 and Figure 2.2.9 show the maximum NH_3 storage capacity of the SCR with temperature increasing for a degreened and an aged SCR sample.
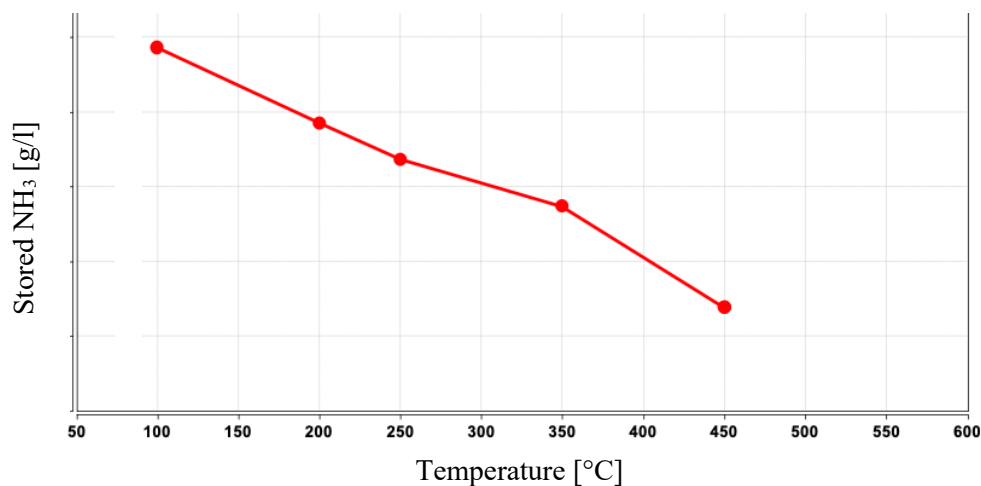
Figure 2.2.8 - NH_3 storage SynGas results (degreened SCR sample)
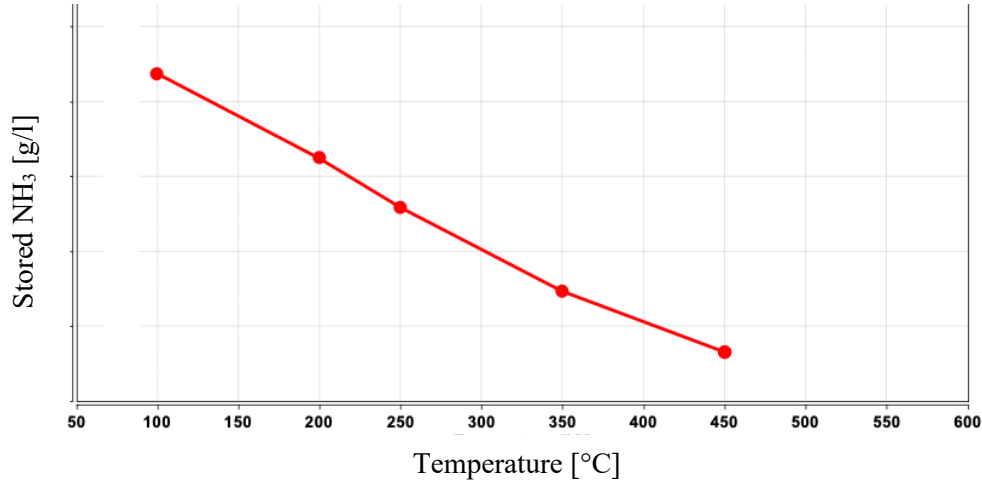
Figure 2.2.9 - NH$_3$ storage SynGas results (aged SCR sample)

In particular, the **NH$_3$ storage capacity** is strongly decreasing with temperature and slightly with ageing. It depends on absorption and desorption reaction rates and gives a temperature dependent steady state equilibrium ammonia loading determined by Arrhenius kinetic coefficients. The NH$_3$ storage reaction rate R$_1$ [mol/m^{2}s] is:

$$R_1 = K_{abs} \cdot c_{NH3} \cdot (1 - \theta_{NH3}) - K_{des} \cdot \theta_{NH3} \qquad (2.8)$$

$$K_{abs} = k_{abs} \cdot e^{-\frac{E_{abs}}{R \cdot T}} \qquad (2.9)$$

$$K_{des} = k_{des} \cdot e^{-\frac{E_{des} \cdot (1 - \varepsilon \cdot \theta_{NH3})}{R \cdot T}} \qquad (2.10)$$

With:

- o   k$_{abs/des}$ → pre-exponential factors
- o   E$_{abs/des}$ → activation energies [J/mol]
- o   ε → shape factor
- o   θ$_{NH3}$ → ammonia surface coverage
- o   c$_{NH3}$ → species concentration.

The parametrization of the NH$_3$ storage model, implemented in the ECU, was done by calibrating these reaction coefficients until the model matches the syngas tests results.

Figure 2.2.10 illustrates syngas tests results used to parametrize the NH_3 oxidation reaction, taking place within the SCR. Tests have been carried out at constant NH_3 concentration.
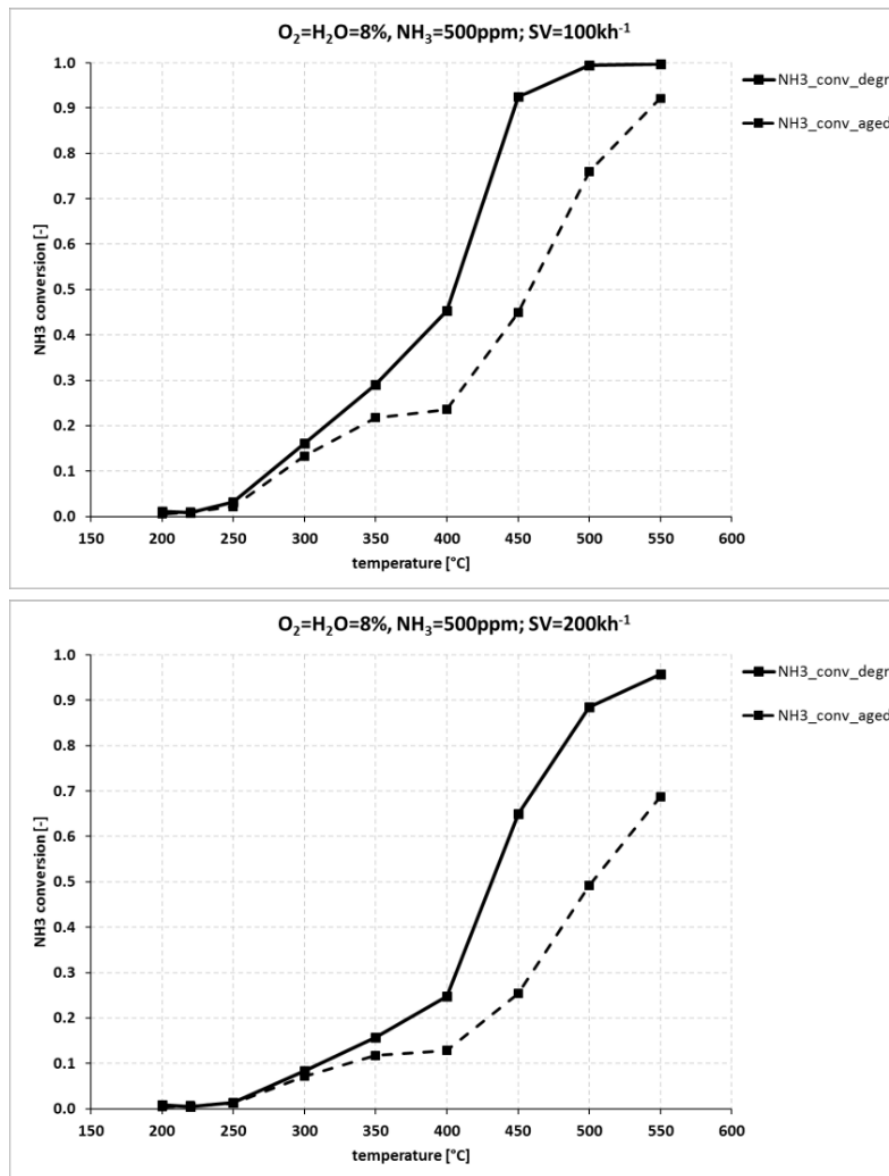
Figure 2.2.10 - SCR NH_3 conversion efficiency vs Temperature at constant SV and NH_3 concentration

The **NH_3 oxidation** reaction (2.7) takes place inside the SCR at a temperature above 250°C. This temperature threshold depends on the SCR substrate material (in this case Cu-Zeolite). When NH_3 oxidation occurs inside the SCR, overdosing is necessary to reach the maximum NO_x conversion efficiency. The activity change at 350-400°C is typical of Cu-Zeolite SCR and it cannot be covered by the existing SCR model. Therefore, the parametrization in this temperature regime was a trade-off between high and low temperature behaviour. The aged SCR shows a lower NH_3 oxidation activity than degreened one.

The three deNO$_x$ reactions (2.3) (2.4) (2.5) of the SCR were parametrized in the ECU model by means of syngas tests results shown in Figure 2.2.11. Tests have been carried out at constant NH$_3$ and NO$_x$ inlet concentrations by varying the SCR temperature and for three different shares of NO$_2$ with respect to that of NO.
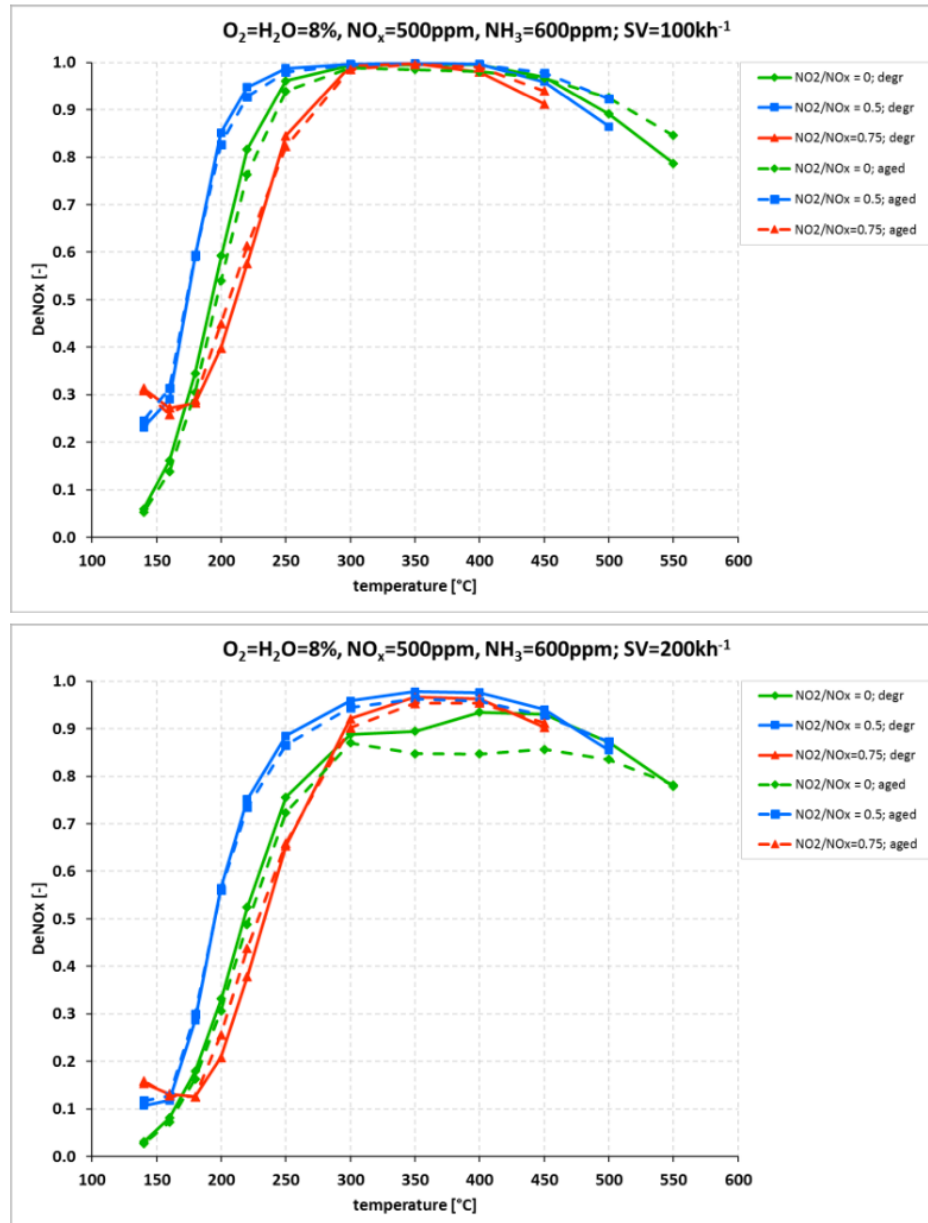
Figure 2.2.11 - SCR NO$_x$ conversion efficiency vs Temperature at constant SV and NO$_x$, NH$_3$ concentrations

The SCR catalyst has shown a good **NO$_x$ conversion efficiency** already at low temperature and low dependency on NO$_2$/NO$_x$ ratio. Efficiency drop is detected above 400°C due to increasing NH$_3$ oxidation. The aged SCR performance is even slightly increasing due to less NH$_3$ oxidation in aged status.

The N_2O formation mechanism inside the SCR was also considered in the parametrization of the model. Syngas tests were carried out at constant NH_3 and NO_x inlet concentrations for different SCR temperatures and three different shares of NO_2 with respect to that of NO. Results are shown in Figure 2.2.12.
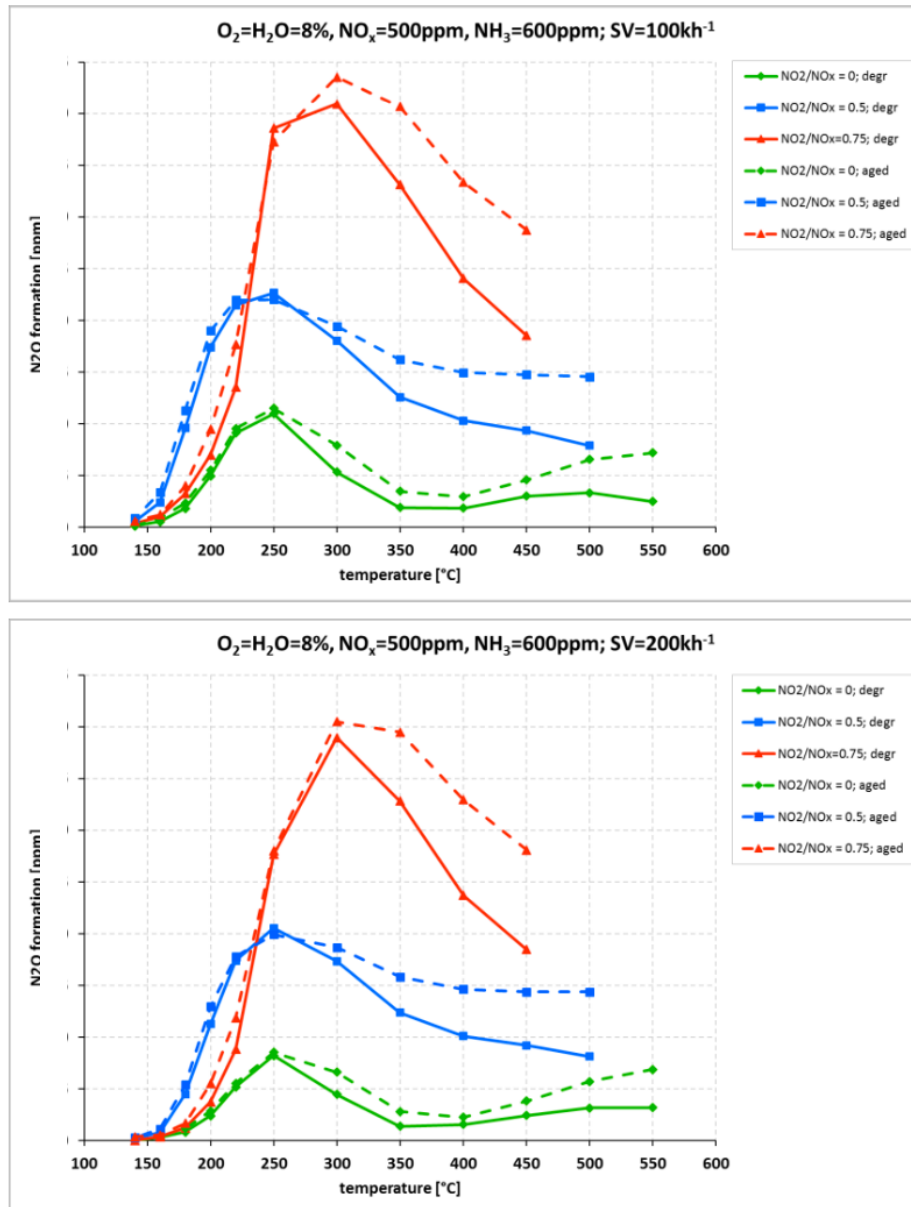
Figure 2.2.12 - SCR N_2O formation vs Temperature at constant SV and NO_x, NH_3 concentrations

N_2O formation (2.6) is strongly depending on the SCR inlet concentrations. It is mainly formed at high NO_2 and NH_3 concentrations and temperatures around 300°C. Aging causes slightly higher N_2O emissions. N_2O formation is almost independent on space velocity because it is mainly produced at the inlet of the catalyst where still high concentrations of NH_3 and NO_x are present.

2.2.3. NH$_3$ storage tests on a real test bench

Purpose of tests

NH$_3$ storage tests have been performed on a real test bench to characterize the SCR storage behaviour when a real exhaust gas flow through it. Tests were carried out on an aged EAS (Worst Case) at different:

- o   SCR inlet temperatures (from 200°C to 550°C; 50°C steps).
- o   Space velocities (30k; 50k; 70k).
- o   Alpha = NH$_3$/NO$_x$ (0.8; 1.0; 1.2; 1.4).

In particular, the aims of tests were:

- o   To compare the actual NH$_3$ storage with the modelled one.
- o   To evaluate the maximum NH$_3$ storage of the real system and its dependency on SCR temperature, space velocity and "α" value.
- o   To evaluate the SCR NO$_x$ conversion efficiency as a function of NH$_3$ storage and its dependency on space velocity, "α" value and SCR inlet temperature.
- o   To define the storage target value to be implemented in the ECU in order to achieve the desired NO$_x$ conversion efficiency while minimizing NH$_3$ slip.

Experimental setup

Test bench layout in Figure 2.2.13 has been adopted during NH_3 storage tests. The engine was equipped with an open ECU that allows online calibration.
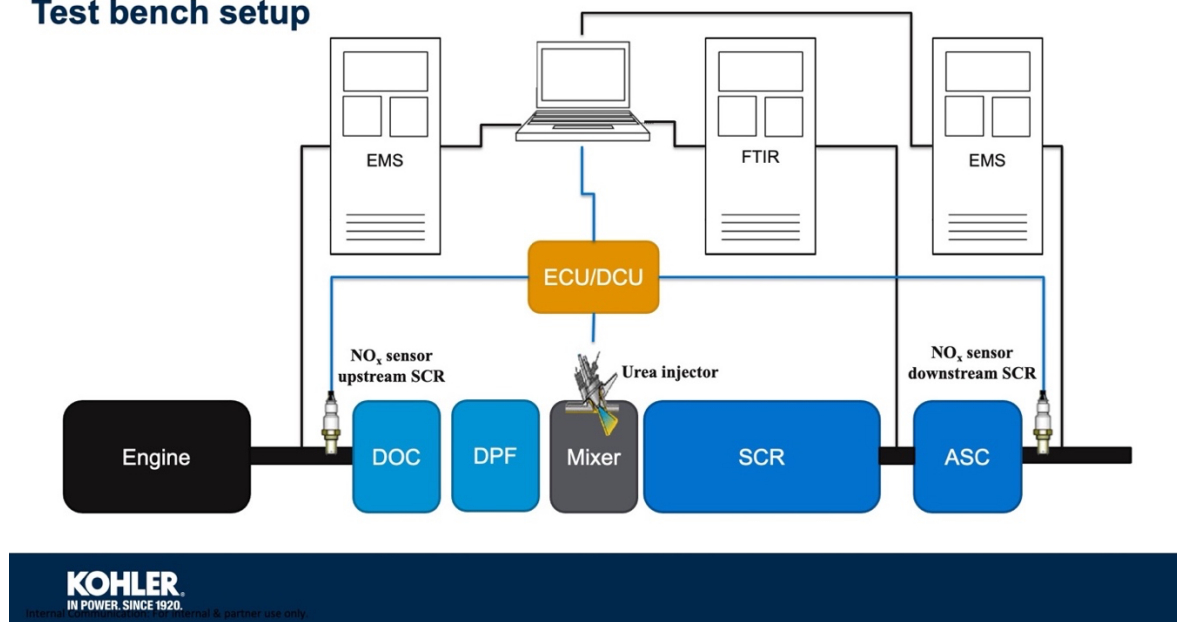
Figure 2.2.13 - Real test bench setup during NH_3 storage tests

The following measurement systems were adopted:

o EMS are able to measure primary pollutant emissions (HC; CO; NO; NO_2) and CO_2. The test bench has been provided with two of them mounted at engine out and tailpipe positions.

o FTIR is adopted to measure ammonia slip. It was mounted at SCR output in order to characterize the only SCR behaviour without considering the ASC influence on NH_3 oxidation

o NO_x sensors have been mounted as in-vehicle configuration. They are not able to distinguish between NO_x and NH_3 emission.

Test Procedure

The adopted test procedure is summarized in the flow chart of Figure 2.2.14.
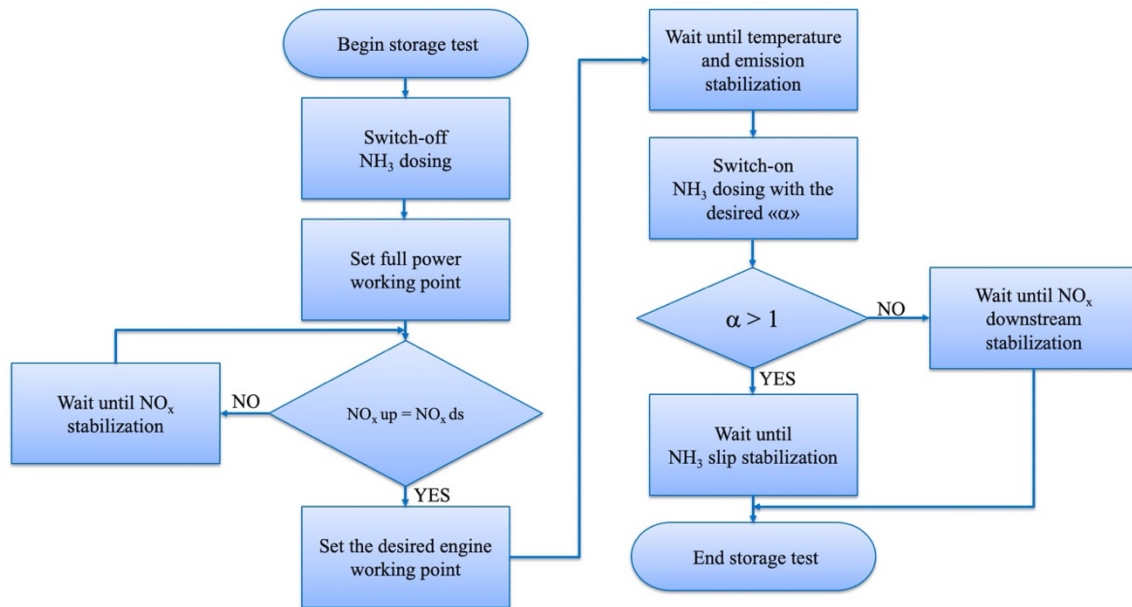
Figure 2.2.14 - Flow chart of NH_3 storage test procedure

The following several steps have been followed:

1. Proper selection of the engine working points to obtain all space velocity and temperature combinations described in Chapter "Purpose of tests".
2. Switch-off dosing.
3. Set full power working point and wait until NO_x downstream become equal to the upstream one. This step was followed to empty the catalyst from NH_3 stored in the previous test.
4. Set engine speed and load as desired.
5. Wait until temperature and emissions stabilization is reached.
6. Set the desired NH_3 dosing by imposing alpha (Open Loop).
7. For alpha > 1 wait until NH_3 slip is stabilized.
8. For alpha < 1 wait until NO_x downstream is stabilized.
9. Turn-off dosing.
10. Wait until NO_x upstream and downstream are equal.

Data analysis
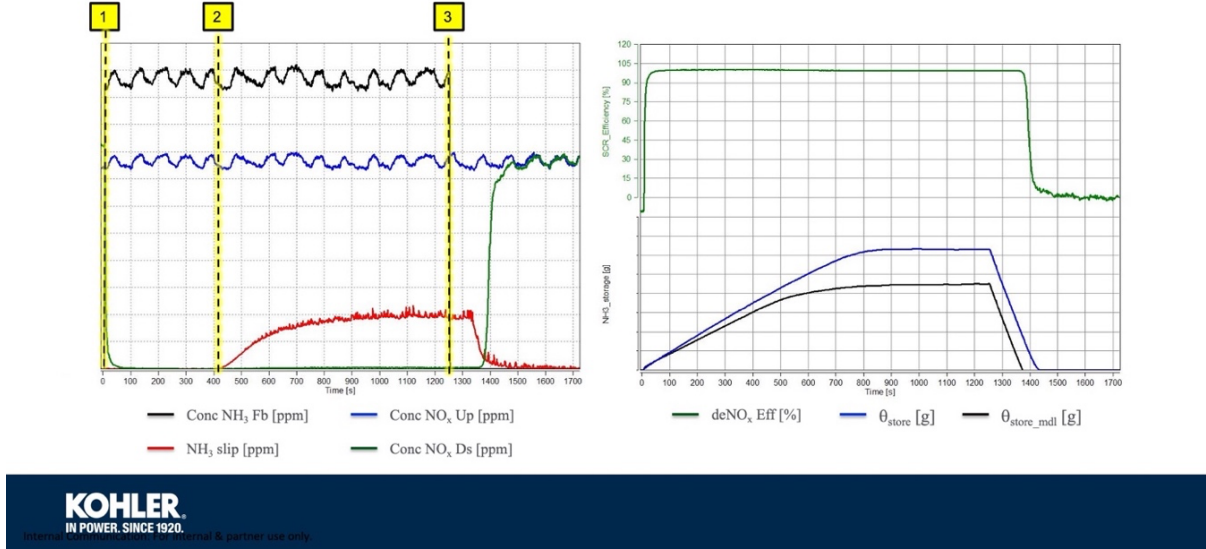
Figure 2.2.15 - Measured and calculated signals to evaluate NH₃ storage tests results

Graphs of this type have been obtained from the test bench data recorder. The one on the left holds measured and ECU signals instead the one on the right contains calculated signals. In the first graph three ranges can be identified:

1- Dosing start (by imposing "α"): previously empty SCR starts to store NH₃ and to convert NO$_x$. NO$_x$ downstream decreases and storage increases.
2- Maximum NH₃ storage and NO$_x$ conversion efficiency are reached.
3- Dosing stop: Stored NH₃ is used to convert NO$_x$ until the SCR is empty.

In the second graph, calculated signals have been computed as follows:

$$\eta_{NO_x} = \left(1 - \frac{concNO_x\_Ds}{concNO_x\_Up}\right) \cdot 100 \qquad (2.9)$$

$$\theta_{store} = \int_{t_0}^{t} G_{NH_3\_store} \cdot dt \qquad (2.10)$$

$$G_{NH_3\_store} = G_{exh} \cdot \frac{concNH_{3\_store}}{3.6 \cdot 10^6} \cdot \frac{\mu_{NH_3}}{\mu_{exh}} \tag{2.11}$$

$$concNH_{3\_store} = concNH_3Fb - concNO_x - concNH_3\_slip \tag{2.12}$$

$$concNO_x = concNO_x\_Up - concNO_x\_Ds \tag{2.13}$$

From graphs of Figure 2.2.15, the maximum NH_3 storage (θ_{store_max}) and θ_{store} to get the desired $deNO_x$ conversion efficiency have been obtained. Although tests were carried out on a real engine, small adjustments have been done in the calculation of the actual NH_3 storage. In particular, the NO_x tailpipe reading of EMS has been aligned with the engine out one when dosing was switched off and the SCR empty. This correction has always been less than 5% (it corresponds to a very small offset since tailpipe emission was always in the order of few ppm when an excess of AdBlue was injected) and can be attributed to the EMS sampling error. The NO_x tailpipe adjustment was done because a very small measurement error becomes very large after the integration operation, due to the long time required to perform a single test. During NH_3 storage calculations, further adjudgments were applied on the injected AdBlue because sometimes the model was not perfectly able to represent the real physical results. In particular, to reach with the real plant a NH_3 storage trend aligned to the modelled one, the injected quantity has been slightly increased during tests performed at high temperature. This adjustment could be justified by the trade-off chosen during the parametrization of the NH_3 oxidation reaction, as described in Chapter "SCR syngas results".

Results

1. Maximum NH₃ storage capacity

The maximum NH_3 storage capacity of the SCR mainly depends on its upstream temperature, as shown both in Figure 2.2.16 and Figure 2.2.17. In particular, the maximum storage capacity decreases with temperature because at high temperature the NH_3 desorption reaction rate increases, shifting the equilibrium between absorption and desorption reactions toward lower NH_3 storage. Solid lines represent results obtained in the real plant while dashed ones correspond to the model results. It is important to note that the model is able to approximate reality well, during both tests at fixed Space Velocity (Figure 2.2.16) and tests at fixed "α" (Figure 2.2.17). This last result has been obtained in all the test performed and therefore the model was validated.
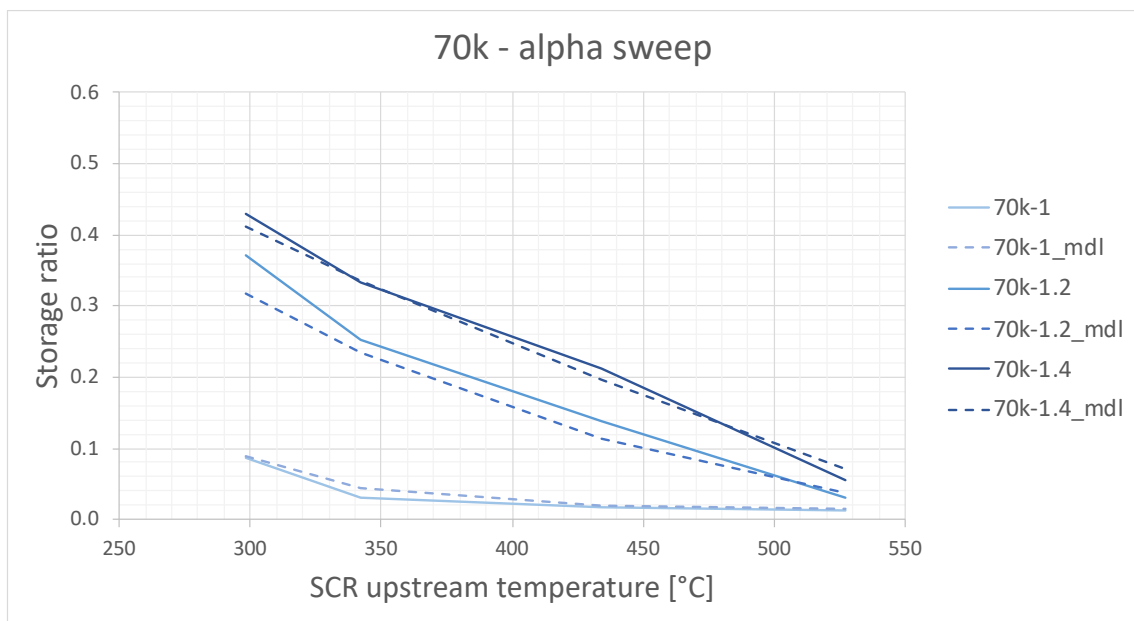
Figure 2.2.16 - Normalized NH_3 storage vs SCR upstream temperature at constant SV

Figure 2.2.16 shows the NH_3 storage versus temperature trend, at fixed Space Velocity and for different values of "α". The NH_3 storage capacity increases with "α" because higher concentration of ammonia enhances weak bounds between NH_3 and the active sites of the catalyst. Modelled and calculated storage when $\alpha \leq 1$ do not represent the maximum because NH_3 concentration is enough to only convert NO_x.

In the graph of Figure 2.2.17, the NH_3 storage versus temperature trend is plotted, at fixed "α" and for different SV values. The maximum NH_3 storage capacity seems to slightly increase with space velocity. This behaviour could be related to the better NH_3 distribution across the inlet section of the SCR while space velocity increases, because a higher SV improves NH_3 mixing with the exhaust flow.
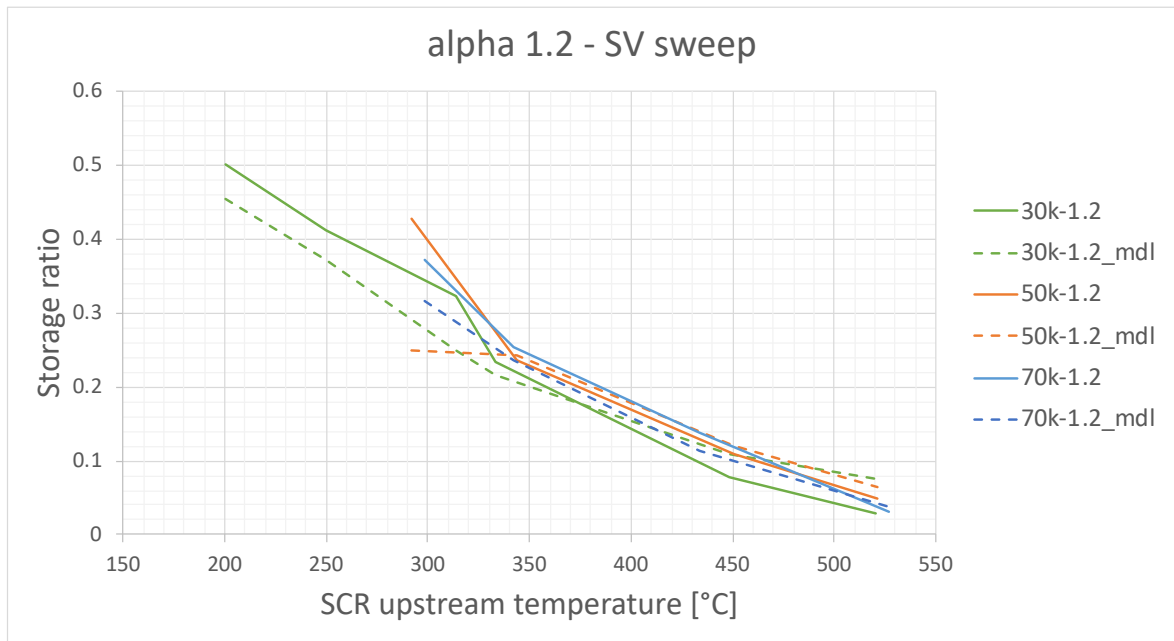
Figure 2.2.17 - Normalized NH3 storage vs SCR upstream temperature at constant alpha

2. NO$_x$ conversion efficiency:

The NO$_x$ conversion efficiency mainly depends on the NH$_3$ stored quantity into the active sites of the SCR, as shown in Figure 2.2.18, Figure 2.2.19 and Figure 2.2.20. A greater amount of stored NH$_3$ increases the NO$_x$ probability of finding a catalyst site in which a NH$_3$ molecule is present, thus improving conversion efficiency.
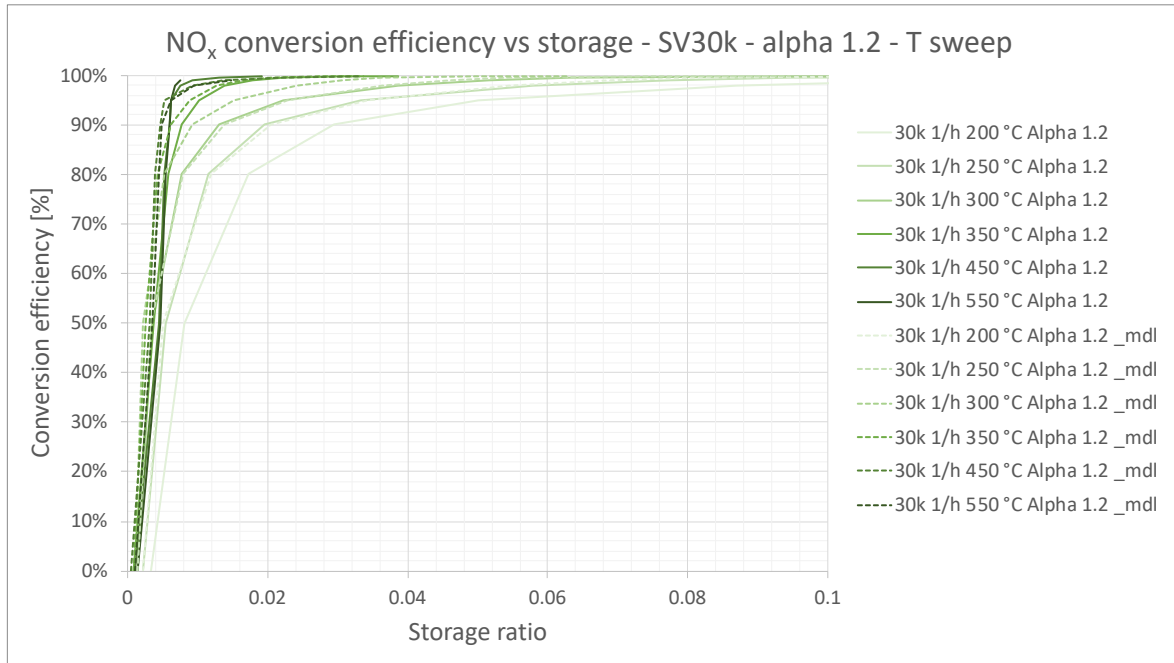
Figure 2.2.18 - NO$_x$ conversion efficiency vs normalized NH$_3$ storage at constant SV and alpha

Figure 2.2.18 shows NO$_x$ conversion efficiency versus NH$_3$ storage trend for different SCR inlet temperature values and fixed SV and "α" ones. The storage required to achieve a certain NO$_x$ conversion efficiency increases as the temperature decreases. The ECU model (dashed lines) shows a lower dependency than measurements.

Figure 2.2.19 shows NO_x conversion efficiency versus NH_3 storage trend for different SV and fixed SCR inlet temperature and "α" values. With increase in space velocity the efficiency lowers, both in calculated and modelled storage. This effect might be related to the shorter time available for $deNO_x$ reactions. To achieve the same NO_x conversion efficiency as at low SV, at higher ones, the NH_3 storage must be greater in order to reach the same probability of finding a catalyst site in which $deNO_x$ reaction can take place.
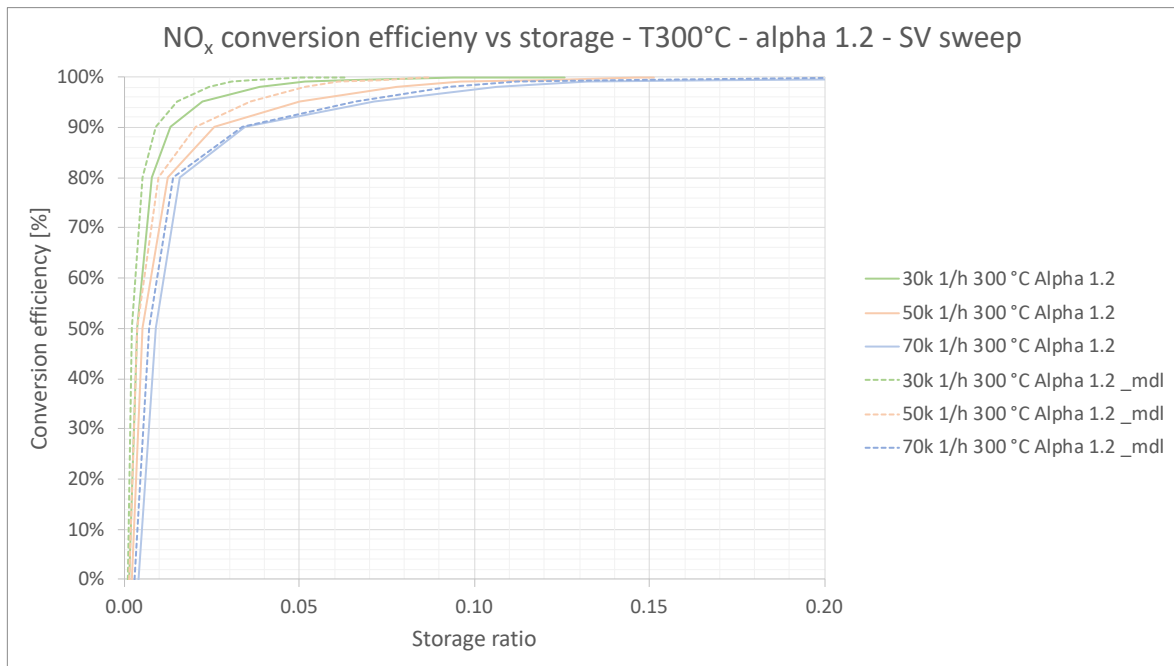
Figure 2.2.19 - NO_x conversion efficiency vs normalized NH_3 storage at constant SCR upstream temperature and alpha

In the graph of Figure 2.2.20, the NO_x conversion efficiency versus NH_3 storage trend is plotted, for different "α" values and fixed SCR inlet temperature and SV ones. By increasing the NH_3 concentration ("α"), the efficiency curve shifts toward higher storage. It seems like weak bounds do not promote $deNO_x$ reactions.
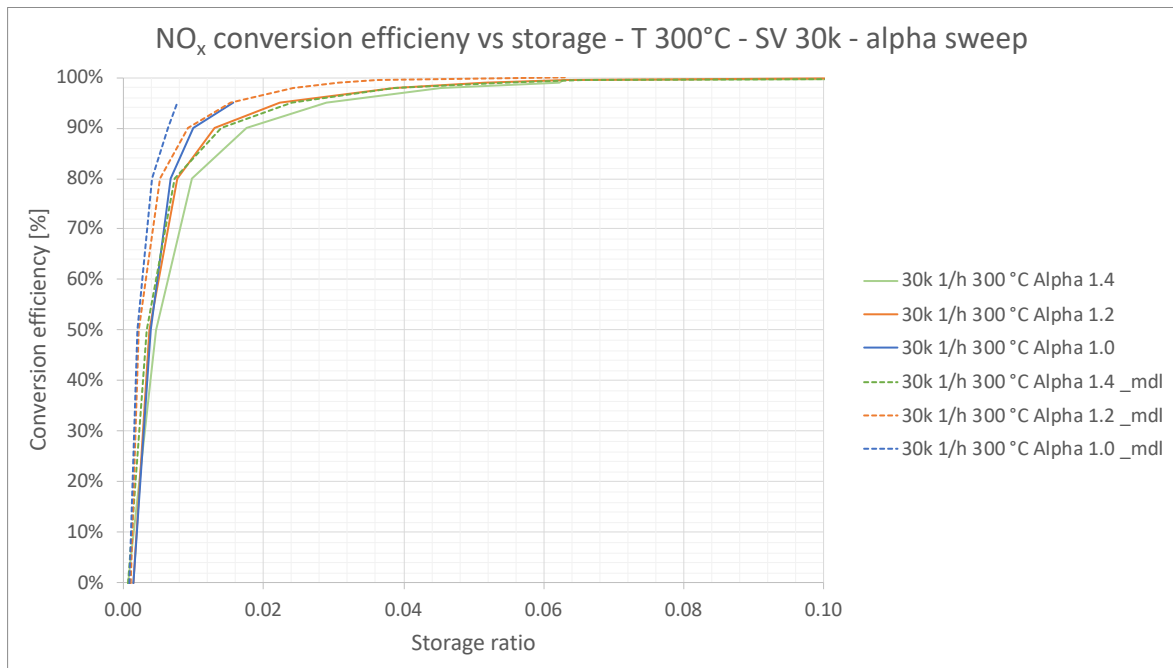
Figure 2.2.20 - NO_x conversion efficiency vs normalized NH_3 storage at constant SCR upstream temperature and SV

As is possible to see from Figure 2.2.16 to Figure 2.2.20, the comparison between measurements (solid lines) and modelled values (dotted lines) is quite good. The differences, which still remain in some cases, have been considered more than acceptable and so the model was considered enough reliable for calibration purposes.

3. Modelled NH₃ storage to achieve different NOₓ conversion efficiency:

Having successfully validated the model and being the closed loop based on it, the storage target in the ECU was defined on the basis of the model results. Modelled NH₃ storage have been plotted as a function of the SCR inlet temperature, for different NOₓ conversion efficiencies and fixed SV, as shown in Figure 2.2.21. In the figure, both the maximum storage and storage curves that allow to achieve a constant NOₓ conversion efficiency are illustrated.
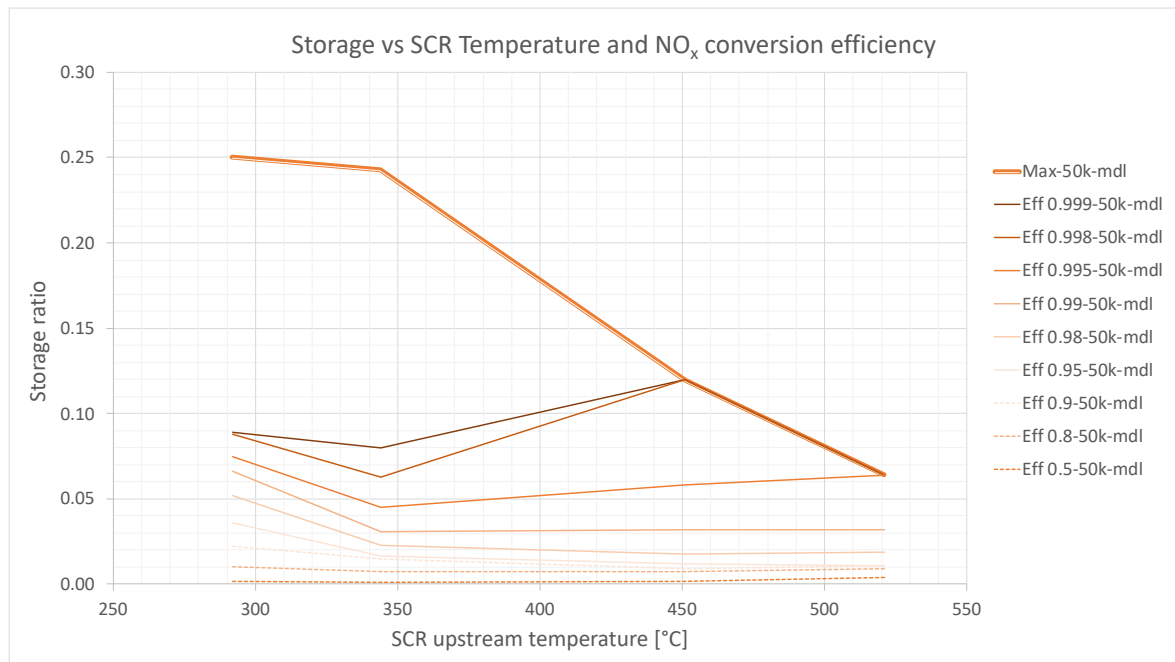
Figure 2.2.21 - Normalized NH₃ storage vs SCR upstream temperature for different NOₓ conversion efficiencies

The curve of maximum NH₃ storage represents a limit not to be exceeded because beyond that, all the extra injected NH₃ becomes NH₃ slip. It is a good practice to keep the distance from the maximum NH₃ storage curve in order to reduce NH₃ slip during temperature transients. It is noteworthy that, at low temperature, a very high NOₓ conversion efficiency is already achieved quite far from the maximum storage curve. At high temperature, on the other hand, to achieve the same NOₓ conversion efficiency, the required storage is closer to the NH₃ maximum storage capacity.

Storage Target definition

The NH_3 storage target map (illustrated in Figure 2.2.22), to be implemented in the ECU, has been chosen starting from NH_3 storage tests results and setting a NO_x conversion efficiency of 99% as first attempt. The first calibration attempt was already able to comply with the emission limits during type approval cycles, but a subsequent refinement was necessary to improve the SCR's behaviour during various maneuvers (such as temperature and SV transients).

		Space Velocity [1/h]															
		0	10000	20000	25000	30000	35000	40000	45000	50000	55000	60000	65000	70000	75000	80000	90000
	0	0.551	0.551	0.551	0.551	0.551	0.551	0.551	0.552	0.552	0.564	0.576	0.588	0.600	0.612	0.624	0.649
	100	0.331	0.331	0.331	0.331	0.331	0.331	0.331	0.332	0.332	0.344	0.356	0.368	0.380	0.392	0.404	0.429
	150	0.242	0.242	0.242	0.242	0.242	0.242	0.243	0.243	0.243	0.255	0.267	0.279	0.291	0.304	0.316	0.340
	200	0.168	0.168	0.168	0.168	0.168	0.168	0.168	0.168	0.168	0.180	0.193	0.205	0.217	0.229	0.241	0.265
	250	0.107	0.107	0.107	0.107	0.107	0.107	0.107	0.108	0.108	0.120	0.132	0.144	0.156	0.168	0.180	0.205
	275	0.082	0.082	0.082	0.082	0.082	0.082	0.082	0.083	0.083	0.095	0.107	0.119	0.131	0.143	0.155	0.180
SCR inlet	300	0.061	0.061	0.061	0.061	0.061	0.061	0.061	0.061	0.061	0.073	0.086	0.098	0.110	0.122	0.134	0.158
Temperature	325	0.043	0.043	0.043	0.043	0.043	0.044	0.046	0.048	0.050	0.058	0.067	0.076	0.084	0.093	0.101	0.119
[°C]	350	0.028	0.028	0.028	0.028	0.028	0.031	0.034	0.037	0.040	0.046	0.052	0.057	0.063	0.069	0.075	0.086
	375	0.017	0.017	0.017	0.017	0.017	0.021	0.025	0.029	0.033	0.036	0.040	0.043	0.047	0.050	0.053	0.060
	400	0.010	0.010	0.010	0.010	0.010	0.014	0.019	0.023	0.028	0.030	0.031	0.033	0.035	0.036	0.038	0.041
	425	0.006	0.006	0.006	0.006	0.006	0.011	0.016	0.020	0.025	0.025	0.026	0.027	0.027	0.028	0.028	0.029
	450	0.006	0.006	0.006	0.006	0.006	0.010	0.015	0.020	0.024	0.024	0.024	0.024	0.024	0.024	0.024	0.024
	480	0.010	0.010	0.010	0.010	0.010	0.014	0.018	0.022	0.026	0.026	0.026	0.026	0.027	0.027	0.027	0.027
	525	0.026	0.026	0.026	0.026	0.026	0.028	0.030	0.033	0.035	0.037	0.039	0.041	0.043	0.045	0.047	0.051
	600	0.078	0.078	0.078	0.078	0.078	0.080	0.083	0.085	0.087	0.089	0.091	0.093	0.095	0.097	0.099	0.103

Figure 2.2.22 – First attempt NH_3 storage target map

At low temperatures, the map in Figure 2.2.22, has been calibrated to require more storage than was actually needed to achieve the desired NO_x conversion efficiency. This was done to improve the $deNO_x$ efficiency performance during a sharp temperature rise.

Storage target refinement

The worst transient maneuver, among those listed in Figure 2.2.23, was found and analyzed to better understand how the NH_3 storage target map had to be refined. From the storage point of view, the fastest temperature transient represents the worst-case maneuver. Although the blue one has reached the highest peak temperature, the red one has been chosen as the worst-case because it shown the highest temperature gradient.

CL_99%	ω [rpm]	Torque [Nm]	T_SCR [°C]	Svel [1/h]	Nox_eff.	NH3_margin	Store_ratio_dmd
from	1400	70	242	17,5	99,8%	100%	0,113
to	1400	full	495	53,7	98,9%	30%	0,033
during						-200,0%	

CL_99%	ω [rpm]	Torque [Nm]	T_SCR [°C]	Svel [1/h]	Nox_eff.	NH3_margin	Store_ratio_dmd
from	1400	70	245	17,5	99,8%	100%	0,114
to	2200	full	473	82,5	97,3%	-10%	0,036
during						-150,0%	

CL_99%	ω [rpm]	Torque [Nm]	T_SCR [°C]	Svel [1/h]	Nox_eff.	NH3_margin	Store_ratio_dmd
from	2200	56	237	35,8	96,6%	100%	0,127
to	2200	full	470	83	97,3%	-10%	0,036
during						-150,0%	

Figure 2.2.23 - NH_3 slip worst case transient maneuver

By controlling the SCR storage target in Closed Loop, it is possible to improve NH_3 slip during SCR temperature transients. Several adjustments on the storage target have been tested and their effects were evaluated.

1. Trying to reduce the storage target at the starting point of the maneuver. No effect was found.
2. Trying to change the storage target depending on SCR temperature trend during transient. The effect was a worst NO_x conversion efficiency and the same NH_3 slip.
3. Trying to reduce the high temperature storage demand (T > 450°C). Results are in Figure 2.2.24 and Figure 2.2.25.
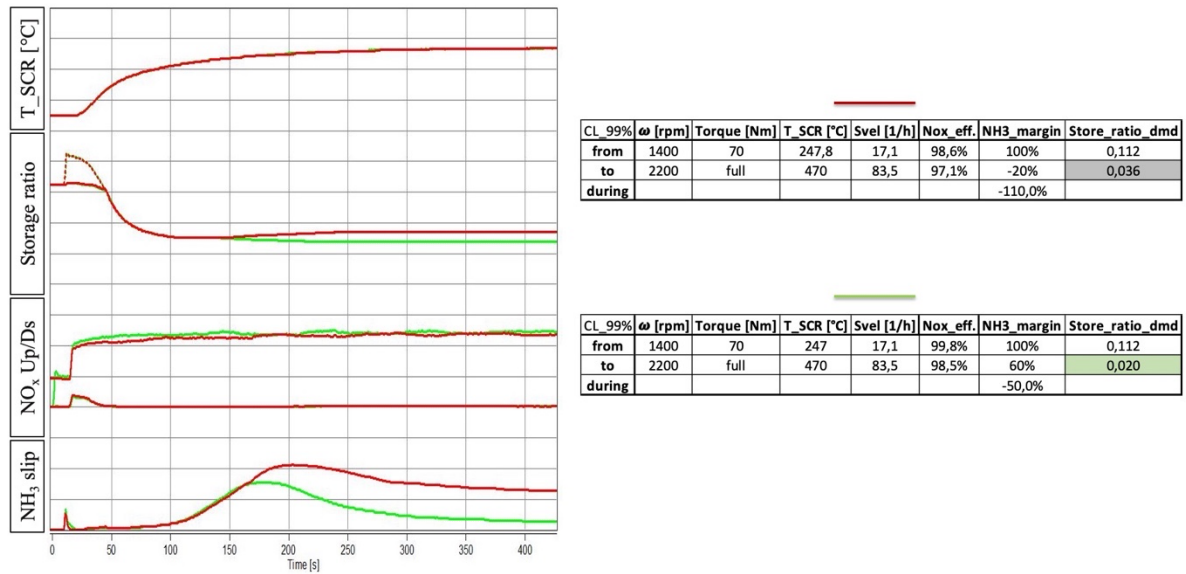
Figure 2.2.24 - NH$_3$ slip improvement on worst case transient maneuver

During the red maneuver of Figure 2.2.23, the third among the three listed adjustment led to an improvement in NH$_3$ slip of 40% without affecting NO$_x$ emissions (results in Figure 2.2.24). The improvement has been confirmed by applying the same adjustment to the blue maneuver of Figure 2.2.23 and results are shown in Figure 2.2.25.
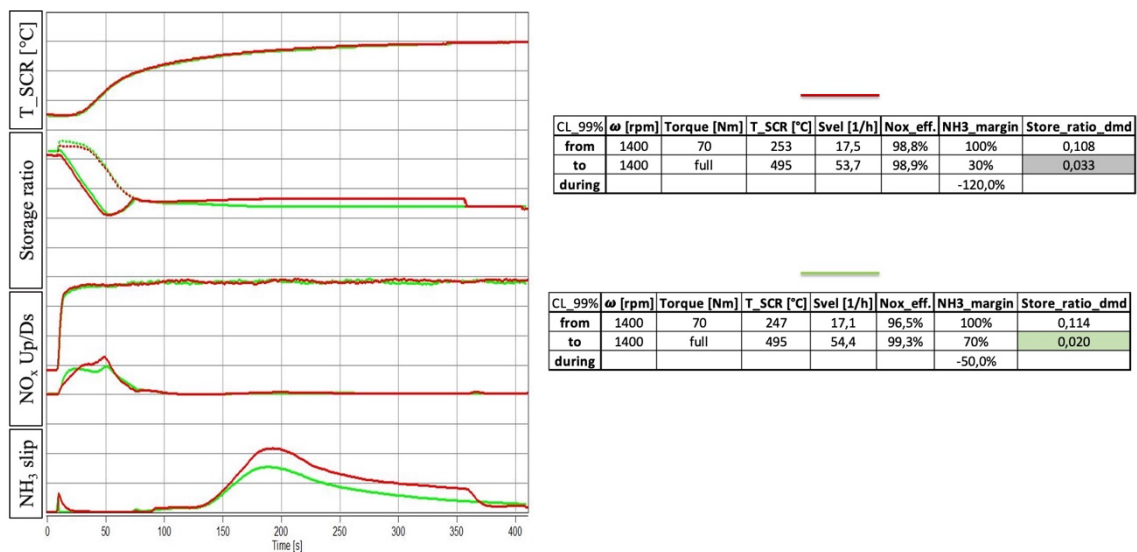
Figure 2.2.25 - NH$_3$ slip improvement validation on another transient maneuver

2.3. Closed Loop Validation

The storage target map has been validated on type approval and customer cycles and the impact of the Closed Loop control strategy was qualitatively demonstrated to be better than Open Loop one when the SCR undergoes temperature transients.

2.3.1. Type approval and customer cycles

NO_x cumulative emission in [g/kWh] and NH_3 average emission in [ppm] were verified to be below targets set by Kohler. Figure 2.3.1 and Figure 2.3.2 show the emission trend on the second NRTC phase with a power setting corresponding to the parent calibration (105kW at 2200 rpm) and aged EAS.
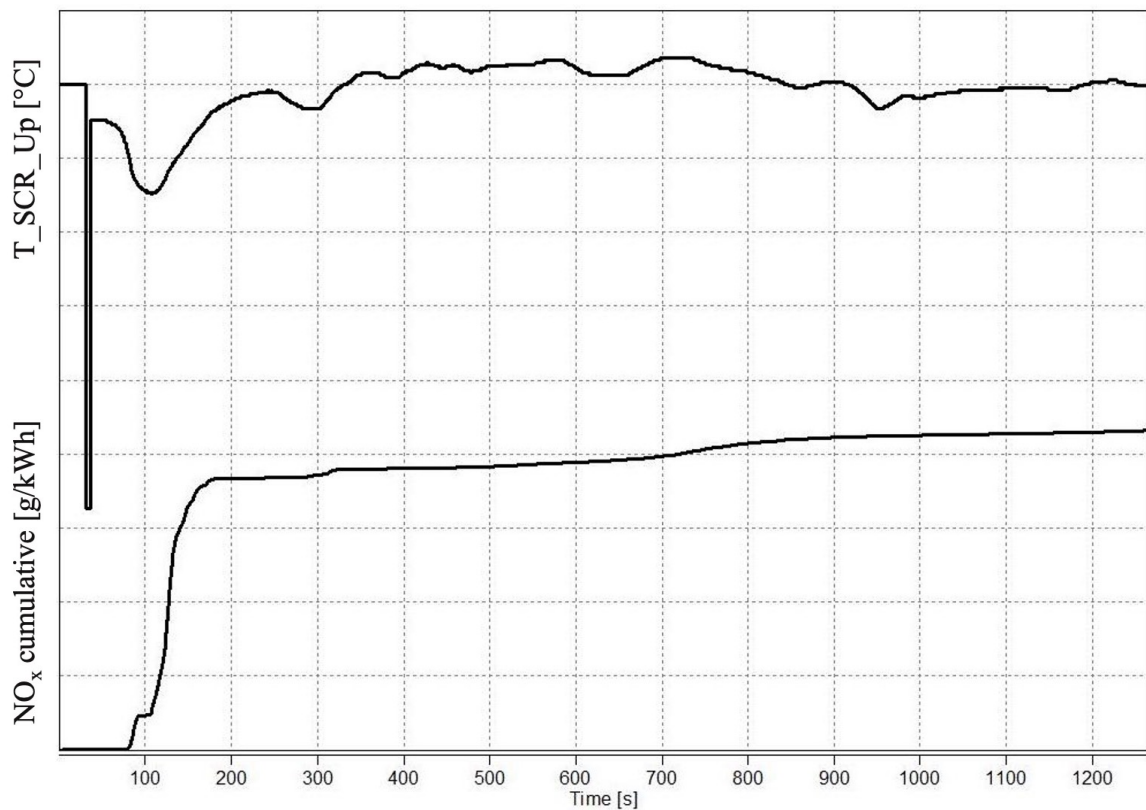
Figure 2.3.1 - NO_x cumulative curve on NRTC type approval cycle (105kW @ 2200rpm)
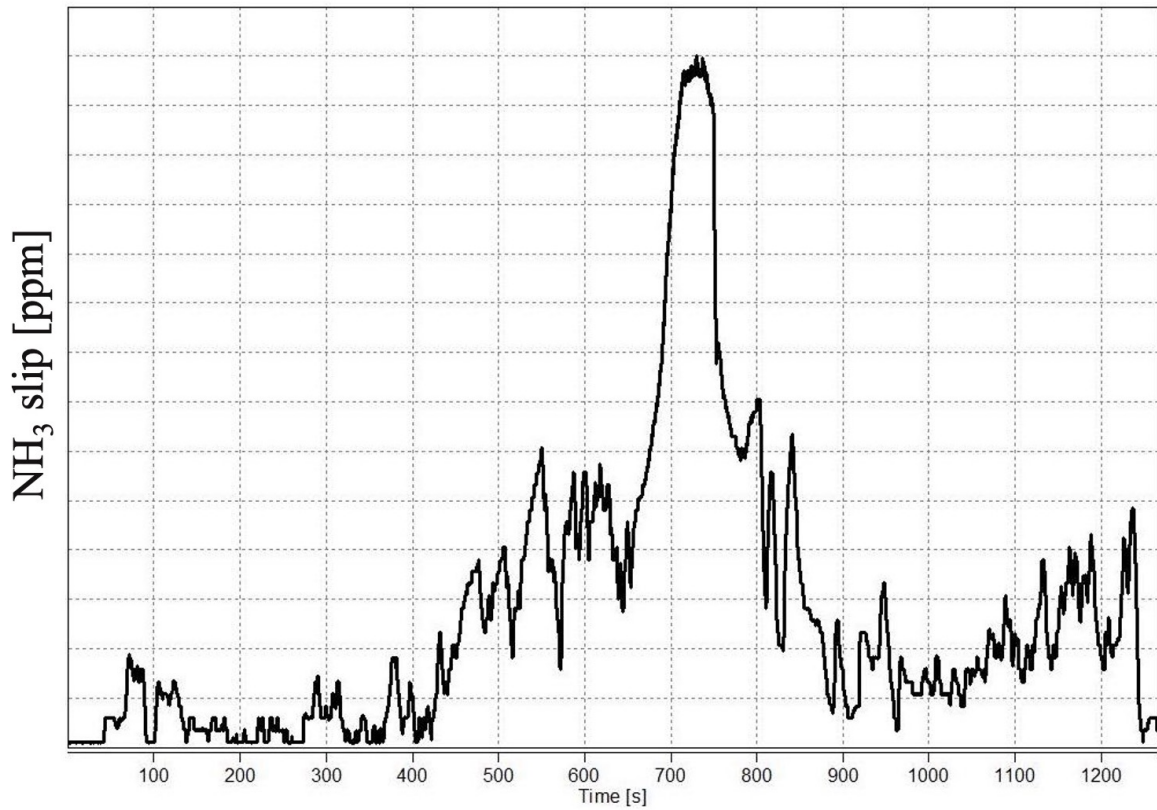
Figure 2.3.2 - NH$_3$ slip on NRTC type approval cycle (105kW @ 2200rpm)

The NO$_x$ cumulative curve is mainly affected by the first few seconds because, although SCR warm-up strategy is already active, the SCR temperature is below the threshold beyond which AdBlue can be injected. Nevertheless, both NO$_x$ cumulative and NH$_3$ average emissions were below targets set by Kohler.

Results on type approval and customer cycles, for the different power settings which have been homologated at the end of this thesis activity, are reported in Table 2.3.1 and Table 2.3.2.

Emission Test Cycles	Aged			Fresh		
	T_SCR_mean [°C]	NOx_cumulative_margin	NH3_average_margin	T_SCR_mean [°C]	NOx_cumulative_margin	NH3_average_margin
NRTC 105kW@2200rpm	291	79%	46%	305	91%	59%
NRTC 75kW@2200rpm	279	84%	61%	279	86%	99%
NRTC 75kW@2500rpm	275	80%	77%	282	86%	98%
RMC 105kW@2200rpm	357	12%	74%	389	46%	76%
RMC 75kW@2200rpm	-	-	-	330	89%	74%
RMC 75kW@2500rpm	316	52%	30%	333	87%	62%

Table 2.3.1 - NO$_x$ cumulative margin for the different engine power levels on type approval cycles

Customer Cycles	Aged			Fresh		
	T_SCR_mean	NOx_cumulative_margin	NH3_average_margin	T_SCR_mean [°C]	NOx_cumulative_margin	NH3_average_margin
LoadAll (3600s)	374	88%	80%	354	96%	76%
Wacker (7800s)	283	96%	73%	270	96%	49%
Superior (8130s)	249	40%	90%	251	78%	40%

Table 2.3.2 - NO$_x$ cumulative margin for the different engine power levels on customer cycles

Emission margins were evaluated with respect to limits set by Kohler. Cycles have been carried out on aged and fresh EAS. It can be notice that the overall performance of fresh EAS is better than aged one, both in terms of NO$_x$ and NH$_3$. During customer cycles, an acceptable and robust margin from Kohler target limits has been reached even tough SCR temperature was very low.

2.3.2. Impact of control strategy

The worst-case maeuver, identified in "Storage target refinement" chapter, has been used to compare different control strategies:

1. **Closed Loop** strategy with a storage target set to achieve **99%** of NO_x conversion efficiency, identified in Figure 2.3.3 with the green colour. It was confirmed being a good solution because it allowed to reach an excellent NO_x conversion efficiency with the lowest NH_3 slip.

2. **Closed Loop** strategy with the **maximum storage** as target, identified in Figure 2.3.3 with the red colour. It has shown the highest NO_x conversion efficiency and the maximum ammonia slip value because the SCR is full of NH_3.

3. **Open Loop** strategy with $\alpha = 1$, identified in Figure 2.3.3 with the blue colour. NO_x conversion efficiency was similar to the closed loop strategy, but it was not possible to optimize NH_3 emission since AdBlue is injected by looking at engine out NO_x emissions.

CL_99%	ω [rpm]	Torque [Nm]	T_SCR [°C]	Svel [1/h]	Nox_eff.	NH3_margin	Store_ratio_dmd
from	1400	70	245	17,5	99,8%	100%	0,114
to	2200	full	473	82,5	97,3%	-10%	0,036
during						-150,0%	

CL_MAX	ω [rpm]	Torque [Nm]	T_SCR [°C]	Svel [1/h]	Nox_eff.	NH3_margin	Store_ratio_dmd
from	1400	70	245	17,1	100,0%	100%	0,356
to	2200	full	473	82,5	99,4%	-200%	0,086
during						-600,0%	

OL	ω [rpm]	Torque [Nm]	T_SCR [°C]	Svel [1/h]	Nox_eff.	NH3_margin	Store_ratio_dmd
from	1400	70	245	17,1	99,3%	100%	
to	2200	full	465	83,3	97,5%	0%	
during						-230,0%	

Figure 2.3.3 - Impact of SCR control strategy on NH_3 slip and NO_x conversion efficiency

By looking at the obtained results in Figure 2.3.3, it is possible to conclude that the closed loop calibration gives the possibility to improve both NO_x conversion efficiency and NH_3 slip avoidance. These tests also confirmed the risk of NH_3 slip when working close to the maximum storage curve.

2.4. NH₃ Adaption strategy

2.4.1. Calibration

The purpose of the strategy is to detect NO_x efficiency drop due to both catalyst aging and sensor/injector drifts. The strategy working principle is summarized in Figure 2.4.1.
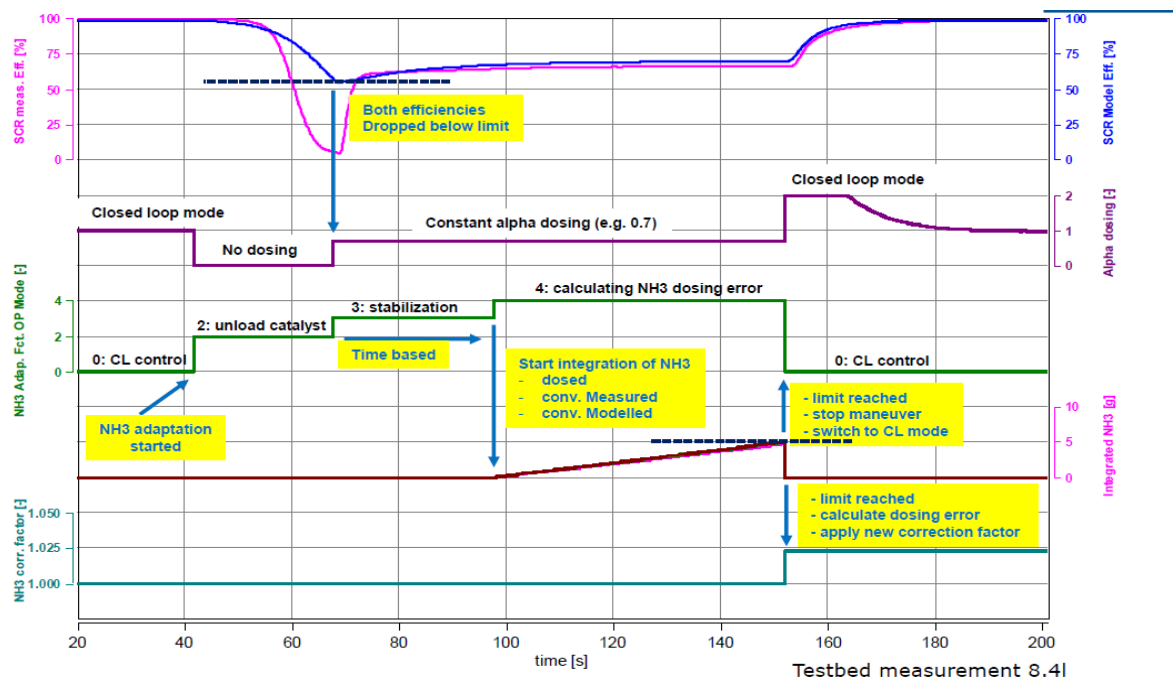
Figure 2.4.1 - NH₃ Adaption strategy working principle

It is implemented in the ECU's software as a state machine, as illustrated in Figure 2.4.2:
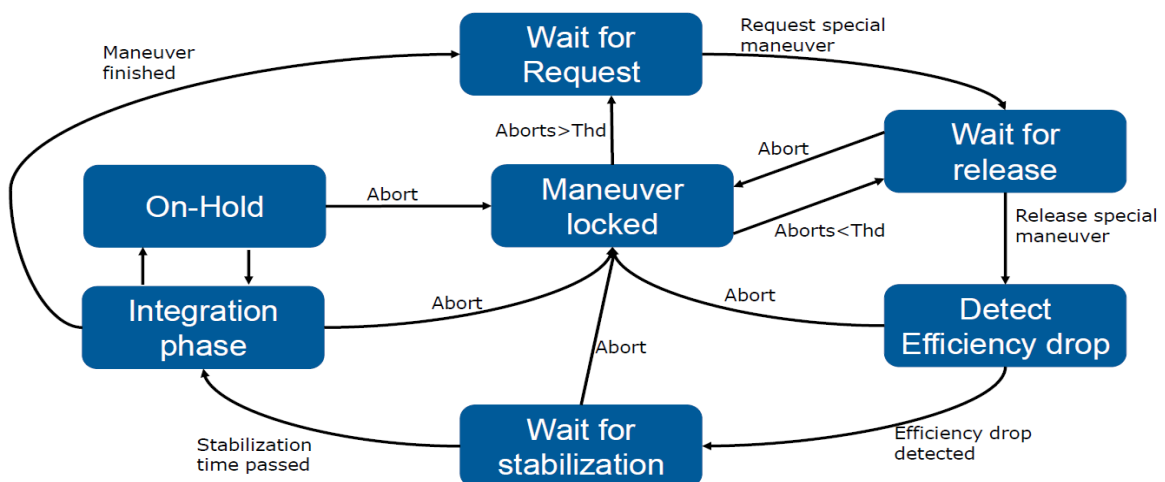
Figure 2.4.2 - NH₃ Adaption strategy state machine

1. Wait for request & **Wait for release**:

The maneuver can be requested in three different manners:

- o Time request
- o After a certain mass of NH_3 has been injected
- o After a certain number of NH_3 slips were detected by the NH_3 slip detection strategy.

It can be released only if several conditions are satisfied. The following variables have to be above a calibratable threshold:

- o Engine Speed
- o NO_x calculated conversion efficiency
- o Upstream measured NO_x
- o NH_3 mass flow
- o SCR temperature.

Furthermore, to release the maneuver, a stationary state needs to be detected. The stationary state detection can be controlled by calibrating a vector in which the difference between the filtered NO_x signal and the actual value coming from the NO_x upstream sensor is present. This calibration lever has been used to prevent the strategy from entering during NRTC because the cycle contains too many temperature and SV transients which therefore lead to unreliable and not robust adaptation results.

2. Detect efficiency drop:

Once the maneuver is released, the efficiency drop detection starts. During this state, the Urea injection is stopped (or reduced, calibratable) and the NO_x efficiency starts to decrease until a lower limit threshold is reached. This state allows to empty the SCR from the NH_3 stored, so that it can be subsequentially be filled in a controlled manner.

3. Wait for stabilization:

Urea injection starts again but in open loop with a calibratable value of "α". For this state, the stabilization time map has been calibrated as a function of SCR temperature and SV. The stabilization time is the waiting time before going to the next state and it is needed to stabilize the system in order to obtain plausible and reliable results.

4. Calculate correction factor:

The following differences are calculated and integrated over time:

- o NO_x sensor upstream - NO_x tailpipe modelled (ASC output)
- o NO_x sensor upstream - NO_x sensor downstream

Integrals are compared with the aim of evaluating the new correction factor to be applied to AdBlue injector.

5. Calculation on-hold:

If the release conditions are not verified, the calculation enters in an on-hold condition in order to wait for the calculation conditions to be validated again and to not lose steps performed up to that moment.

6. Maneuver locked:

If either the special maneuver is switched off or the timeout is reached, the maneuver is aborted.

2.4.2. Validation

Adaption strategy has been activated, for the first time, during this thesis project. Hence, it required a robust validation procedure made by the following steps:

1. To evaluate the influence of the engine working point on the adaption strategy

Tests NH3_Adn Calibration						
Speed [rpm]	Torque [Nm]	T_SCR [°C]	SV [1/h]	Exp_Corr_Fact	Corr_Fact	Stabilization_time [s]
1600	160	300	30000	1.000	1.040	45.0
2200	150	300	50000	1.000	1.003	58.5
2200	250	300	72000	1.000	0.960	58.5
2000	230	315	56400	1.000	0.970	59.8
2000	340	350	70000	1.000	0.956	40.0
2500	full	385	85000	1.000	0.960	26.0
1150	425	450	30000	1.000	1.008	58.5
1400	535	450	50000	1.000	0.985	58.5
1900	480	450	70000	1.000	0.970	40.0
1000	full	530	25000	1.000	1.013	40.0
1800	full	540	70000	1.000	1.025	26.0
2200	full	490	80000	1.000	1.004	26.0

Table 2.4.1 - NH$_3$ Adaption correction factor as a function of the engine working point

Although the expected correction factor was equal to unity, the average value of these tests was slightly different due to the normal and accepted dispersion of the EAS manufacturing process. The error of the strategy as a function of the engine working point has been considered acceptable.

2. To deviate AdBlue injector:

AdBlue injector deviation							
				Injector (-10%)		Injector (+10%)	
Speed [rpm]	Torque [Nm]	T_SCR [°C]	SV [1/h]	Exp_Corr_Fact	Corr_Fact	Exp_Corr_Fact	Corr_Fact
1600	160	300	30000	1.100		0.900	
2200	150	300	50000	1.100	1.110	0.900	0.907
2200	250	300	72000	1.100		0.900	
2000	230	315	56400	1.100		0.900	
2000	340	350	70000	1.100		0.900	
2500	full	385	85000	1.100	1.048	0.900	0.850
1150	425	450	30000	1.100		0.900	
1400	535	450	50000	1.100		0.900	
1900	480	450	70000	1.100	1.067	0.900	0.874
1000	full	530	25000	1.100	1.084	0.900	0.902
1800	full	540	70000	1.100		0.900	
2200	full	490	80000	1.100	1.077	0.900	0.889

Table 2.4.2 - NH$_3$ Adaption correction factor with a deviated DEF injector

The injector has been deviated in both directions (+/-10%) and the NH$_3$ adaption strategy was always able to recover the deviation with a proper amount, making a very small error. Results in Figure 2.4.3.
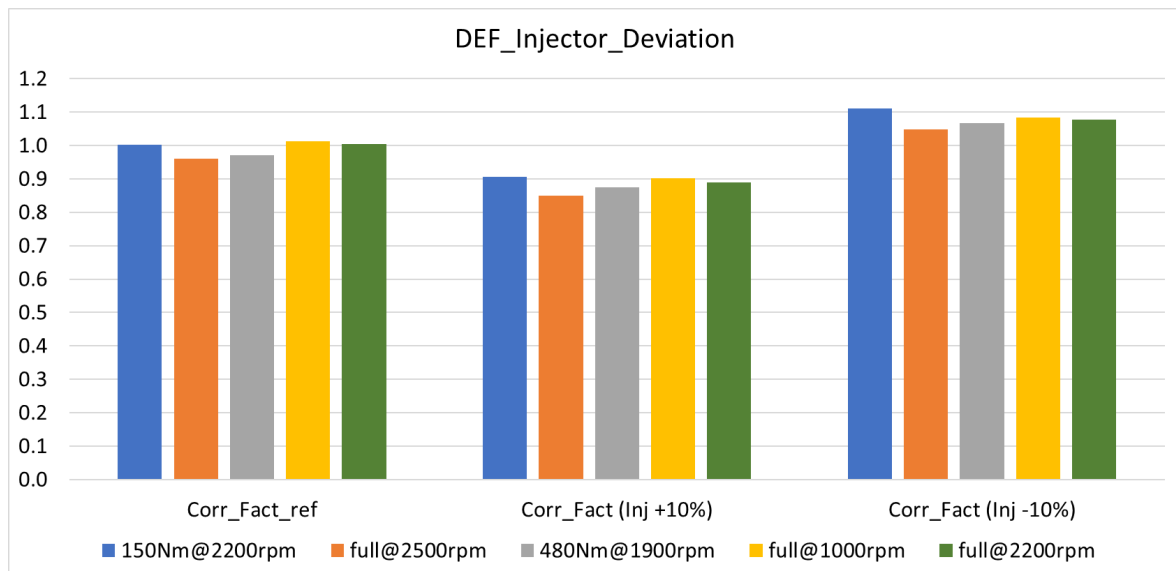
Figure 2.4.3 - Bar graph of NH$_3$ Adaption correction factor with and without a deviated DEF injector

2. To deviate upstream NO_x sensor:

NOx sensor upstream deviation							
				NOx (+10%)		NOx (-10%)	
Speed [rpm]	Torque [Nm]	T_SCR [°C]	SV [1/h]	Exp_Corr_Fact	Corr_Fact	Exp_Corr_Fact	Corr_Fact
1600	160	300	30000	1.096	1.134	0.904	0.869
2200	150	300	50000	1.106	1.159	0.894	0.857
2200	250	300	72000				
2000	230	315	56400				
2000	340	350	70000				
2500	full	385	85000	1.105	1.087	0.895	0.822
1150	425	450	30000				
1400	535	450	50000				
1900	480	450	70000	1.094	1.084	0.906	0.834
1000	full	530	25000				
1800	full	540	70000				
2200	full	490	80000	1.101	1.141	0.899	0.841

Table 2.4.3 - NH_3 Adaption correction factor with a deviated NOx engine out sensor

The upstream NO_x sensor has been deviated in both directions (+/- an offset corresponding to about +/-10%) and the correction factor have always gone in the expected direction. It is important to note that a deviation of 10% of the measured NO_x does not correspond to an error of 10% on the injected NH_3.

3. To verify that the strategy does not take place during NRTC cycle.

Several calibration loops were carried out, modifying the release condition of the strategy when a transient is detected, so as to avoid its entry during NRTC.

4. To determine the strategy effectiveness in recovering the EAS manufacturing process variability:

During the validation activity of the Closed Loop dosing control strategy, slightly different behaviors were noted between different SCR catalysts, in terms of NO_x conversion efficiency and NH_3 slip. These differences were related to EAS and DEF injector manufacturing process variability. By activating the NH_3 adaption strategy, it was possible to reduce these differences and to obtain more aligned and robust emission performance. Figure 2.4.4 shows the SCR behaviour before adaption in red and after adaption in blue. The NO_x tailpipe emission is referred to the one measured by the downstream NO_x sensor.
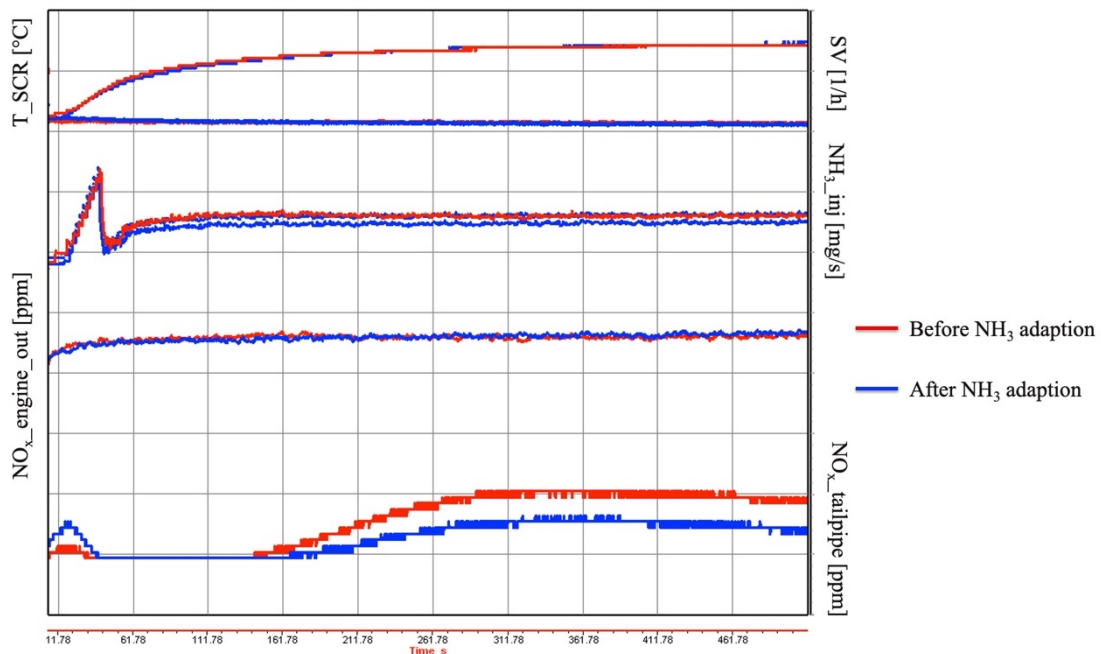

Figure 2.4.4 - NH_3 adaption results with a SCR different from the one used to calibrate the target storage map

A FTIR measurement system, mounted in tailpipe position, has measured a reduction of NH_3 slip and an increase in NO_x conversion efficiency at the end of the adaption. This measurement proved that the higher NO_x concertation, measured by the downstream sensor before adaption, was mainly affected by the presence of NH_3 slip. In fact, the onboard NO_x sensors measure every nitrogen-based compound and are not able to split the contribution of NO_x from the one of NH_3.

2.5. NH₃ Slip Detection strategy

2.5.1. Calibration

The NH$_3$ slip detection strategy is aimed at recognizing any excessive tailpipe NH$_3$ emission. The onboard downstream NO$_x$ sensor measures every nitrogen-based compound. The present software strategy is needed in order to distinguish NH$_3$ from NO$_x$ emissions. It is based on the principle that the SCR catalyst has a different filtering behavior on NH$_3$ and NO$_x$ emissions. The strategy working principle is shown in Figure 2.5.1.
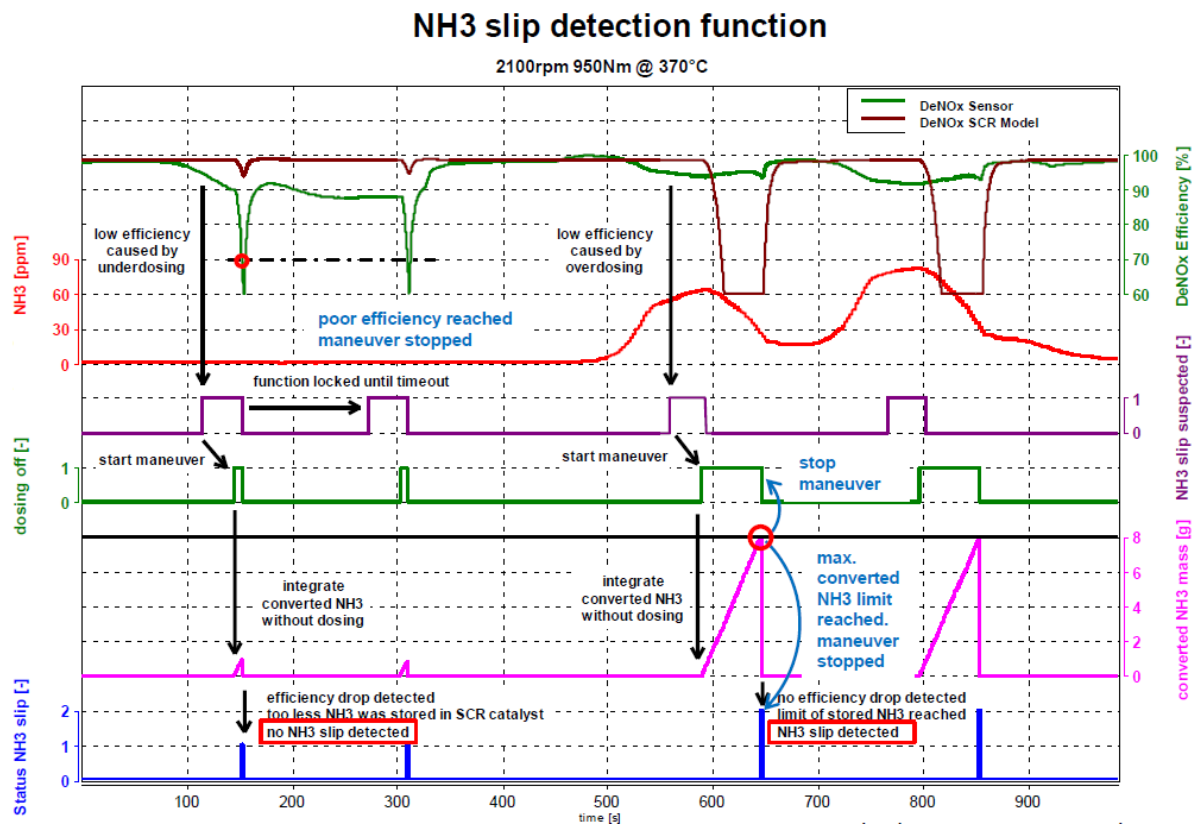

Figure 2.5.1 - NH$_3$ Slip Detection strategy working principle

There are two possible reasons for a lower measured NO$_x$ conversion efficiency compared to the modelled one:

o Too less NH$_3$ dosing into the SCR system
o Too much NH$_3$ dosing into the SCR system and therefore NH$_3$ slip.

To overcome the cross sensitivity of the NO_x sensor, NH_3 dosing is either switched off or switched to a very low dosing and the sensor response is observed. Two possible situations can arise after switching off the dosing:

- o The calculated $deNO_x$ efficiency drops down. Cause can be related to a low quantity on NH_3 introduced into the catalyst
- o The calculated $deNO_x$ efficiency keeps high for a certain time. This behaviour is due to NH_3 slip.

There is no state machine governing this strategy, so values are computed at each ECU task. The main steps of the maneuver are the following:

1. Detect if the calculated efficiency is much lower than modelled one

The maneuver is released if the following conditions are verified:

- o The modelled NO_x conversion efficiency is above a calibratable threshold. This calibration lever has been also used as a smart way to inhibit the strategy when results could be not reliable (e.g.: at very low SCR temperature and during regeneration, when the temperature reaches 600°C)
- o The ratio between the calculated and modelled $deNO_x$ efficiencies is below a calibratable threshold
- o A calibratable time interval is elapsed since the last slip detection
- o The temperature rise of the SCR catalyst has to be lower than a calibratable limit.

2. Disable Dosing

The request to switch-off or reduce dosing is set once the maneuver is released. The maneuver is stopped if:

- o The measured $deNO_x$ efficiency is below a threshold. That basically means that the SCR catalyst doesn't have stored NH_3 anymore
- o The actual operating mode doesn't allow a NH_3 slip detection event.

If the maneuver is started, a calibratable value of "α" is used as NH_3 dosing request. In this project, it was chosen to switch-off the dosing.

3. Model and efficiency decrease when dosing is down

The amount of NO_x mass upstream the EAS system and the downstream one are integrated. At the end of the maneuver the integrators are reset to 0 until the next maneuver starts.

4. Detect if Slip is present according to calculated and modelled efficiency (integrated masses comparison step)

The difference between the NO_x mass upstream and the NO_x mass downstream is the amount NH_3 stored in the catalyst, if NH_3 oxidation were neglected. If the stored NH_3 mass is above a limit it is assumed that the SCR/ASC catalyst loading was very high and therefore the previously detected low $deNO_x$ efficiency was caused by NH_3 slip. A counter is updated once NH_3 slip is detected.

2.5.2. Validation

The aim of validation was to verify the strategy's ability of detecting NH_3 slip during type approval cycles. Ammonia slip has been obtained by deviating the DEF injector.
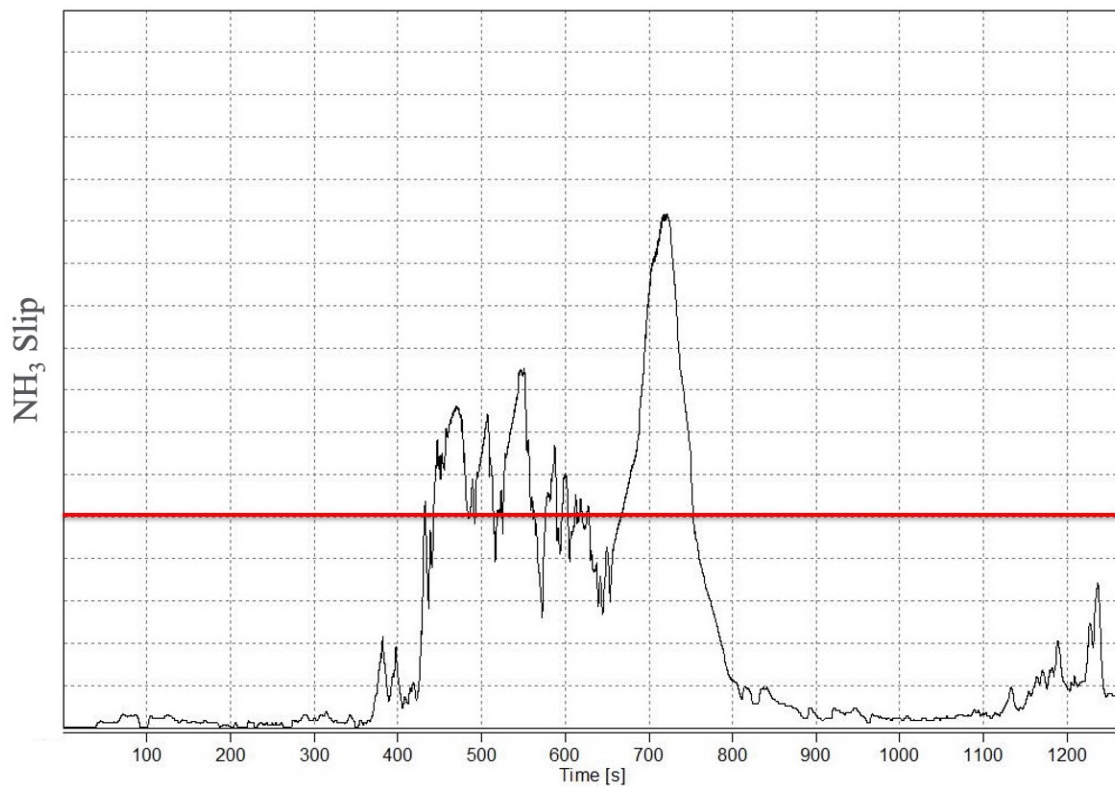
1. NRTC

Figure 2.5.2 - NH_3 Slip over the second NRTC phase with deviated DEF injector

Figure 2.5.2 refers to the second NRTC phase. The strategy has been calibrated, in steady state operating conditions, to detect NH_3 slip when the red threshold was overcoming.
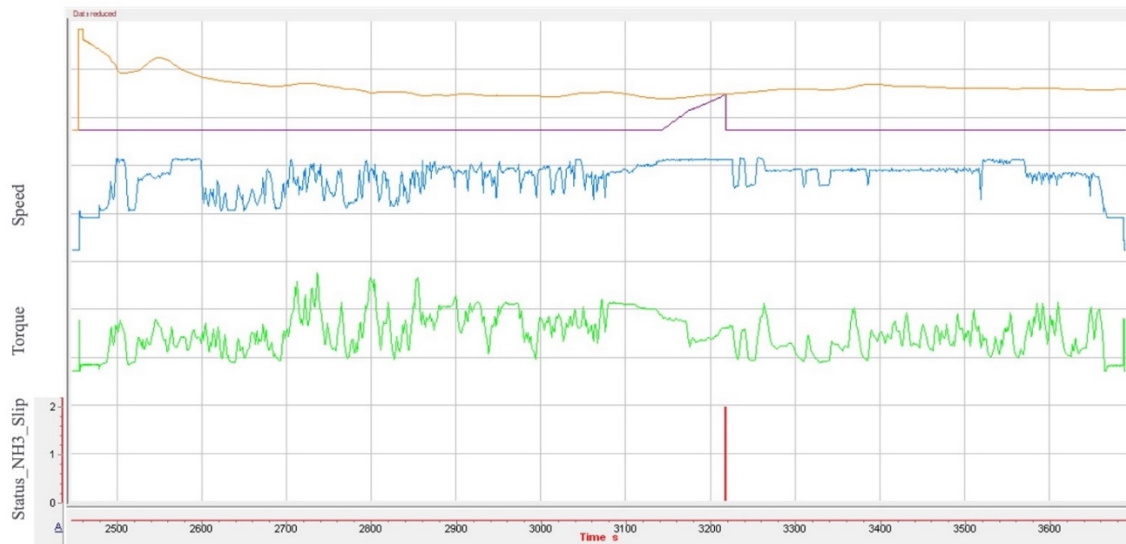
Figure 2.5.3 – NH$_3$ Slip Detection strategy validation over the second NRTC phase with deviated DEF injector

The strategy was able to detect NH$_3$ slip only once during NRTC because this cycle is far from being stationary. NH$_3$ slip detection can be monitored by looking at the "Status NH$_3$ slip" variable in Figure 2.5.3. In particular:

o   Status NH$_3$ slip = 1 → Efficiency drop due to insufficient NH$_3$ storage in the SCR.
o   Status NH$_3$ slip = 1 → Efficiency drop due to high NH$_3$ storage in the SCR.
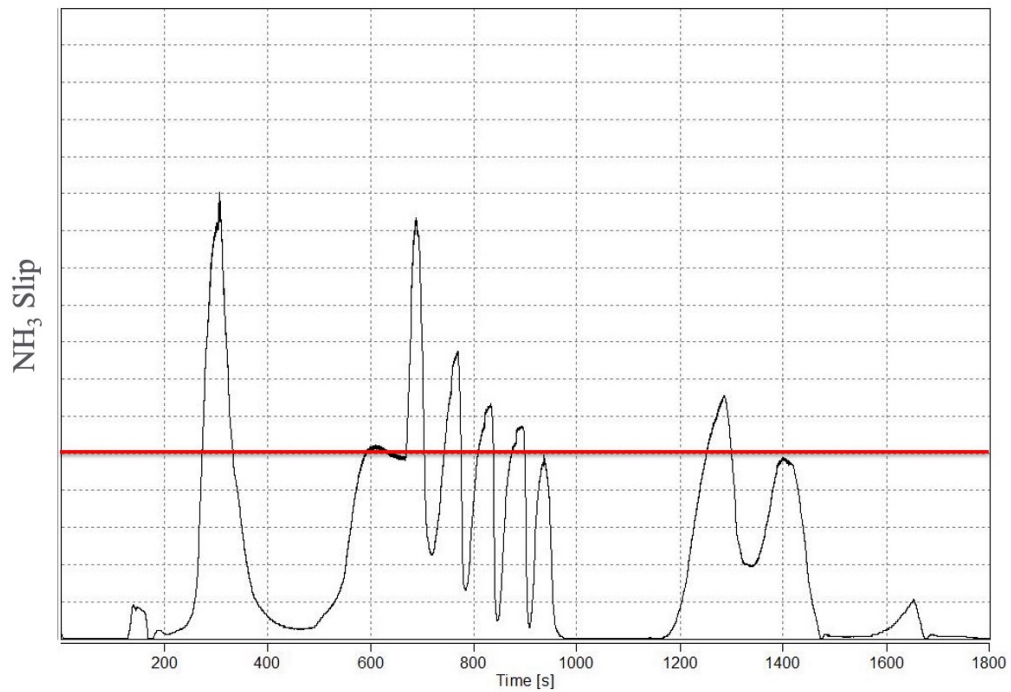
2. RMC

Figure 2.5.4 - NH$_3$ Slip over the RMC with deviated DEF injector
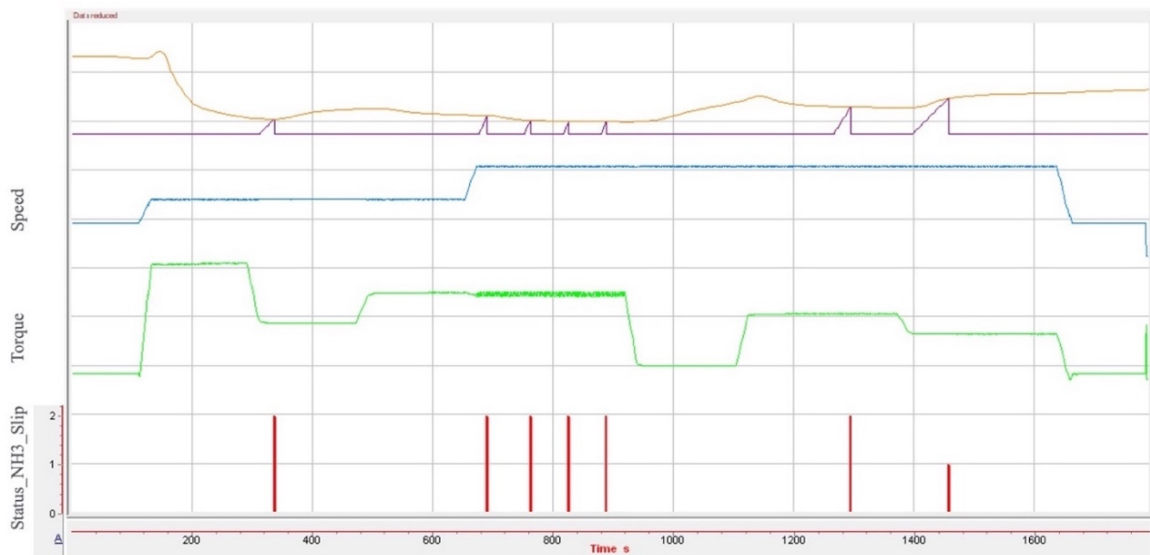

Figure 2.5.5 - NH$_3$ Slip Detection strategy validation over RMC with deviated DEF injector

As shown in Figure 2.5.4, the calibrated threshold beyond which the strategy should work, was exceeded 6 times and the strategy was perfectly capable of detecting NH$_3$ slip whenever this threshold was crossed. NH$_3$ slip detection can be monitored by looking at the "Status NH$_3$ slip" variable in Figure 2.5.5.

3. Conclusions

The SCR Closed Loop DEF dosing control strategy has been chosen to improve NO_x conversion efficiency and NH_3 slip over the whole SCR temperature operating window, in particular at low temperature and during temperature transients. The Closed Loop strategy is based on the error between target and modelled NH_3 storage inside the SCR. Being NH_3 storage a non-measurable quantity, it is calculated by the ECU based on SCR reactions rates. These reactions rates were parametrized and implemented inside the ECU by a Kohler supplier after having performed several tests on a SynGas test bench. To validate the NH_3 storage model, tests have been performed on a real engine mounted on a Kohler's test bench. These tests have been carried out in steady state engine operating conditions, injecting DEF in open loop (by imposing "α") and measuring SCR downstream NH_3 slip and tailpipe NO_x emissions. Test recorders have been processed and the actual NH_3 storage was compared with the modelled one. Once the NH_3 storage model has been validated, test results were further processed to choose the storage target to be implemented in the ECU in order to obtain a NO_x conversion efficiency close to 90% while reducing NH_3 slip. Storage tests have shown results with a trend similar to the literature ones. The implemented storage target map as a function of SV and SCR inlet temperature has been validated over temperature transients, type approval and customer cycles, refining the calibration when needed.

Finally, NH_3 adaption and slip detection strategies have been calibrated and validated to take into account EAS aging and DEF injector/NO_x sensors drifts. These strategies can be of particular importance also for fresh EAS because they are able to absorb EAS differences related to the manufacturing process variability.

The electronic control strategies here developed, have allowed the optimization of the SCR performance. The engine was able to comply with the current emission legislation and has been homologated with success.

Future developments will be on testing and validation of the adaption and the NH_3 slip detection strategies for real applications, monitoring data fleet and understanding the robustness of these two specific new functionalities.

4.   References

[1]   S. D'ambrosio, Course of Combustion Engines and their Application to Vehicle, Turin, 2019.

[2]   G. Ferrari, Motori a combustione interna, Il Capitello, 2005.

[3]   J. B. Heywood, Internal Combustion Engine Fundamentals, Mc Graw Hill, 2018.

[4]   F. Millo, Course of Engine Emissions Control, Turin, 2019.

[5]   Bosch, Automotive Mechatronics, Springer Vieweg.

[6]   F. Siccardi, Engine calibration in a virtual envirorment, 2018.

[7]   "DieselNet," [Online]. Available: https://dieselnet.com/standards/.

[8]   I. Nova and E. Tronconi, Urea - SCR Technology for deNOx After Treatment of Diesel Exhaust, Springer, 2014.

[9]   M. Caggiano, Corso di Alta Formazione in Calibrazione Motopropulsore, FEV, 2015.

[10] E. Corti, Corso di Alta Formazione in Calibrazione Motopropulsore, 2015.

[11] R. A. Alberty and R. J. Silbey, Physical chemistry, New York: Wiley, 1997.

[12] D. W. Green and R. H. Perry, Perry's Chemical Engineers' Handbook, Mc Graw Hill, 2007.

[13] Bosch Professional Automotive Information, Diesel Engine Management Systems and Components, Springer Viewing, 2014.

5. Acknowledgements

First of all, I am very grateful to Kohler Engines EMEA for giving me the possibility to write my Master Thesis, providing the resources and knowledge for successfully complete the work.

I would like to hugely thank my company supervisors Simone R. and Fabio S., for the brilliant support, not only from technical side but also from human side, which was essential during the hard times due to Covid19.

To professor Millo, for the support during the thesis period and for making this experience possible at Kohler Engines EMEA.

A special thanks goes to my life partner, for believing in me and giving me the strength to go on even in the most difficult moments.

To my father, my mother and my sister, for their psychological and economic support and for allowing the realization of my greatest dream, that of becoming an engineer.

To my friend Calogero, for giving me a friendship that I had never had before and for always supporting me.

To Leonardo, Riccardo, Francesco, Giuseppe and Vito, for giving me unforgettable moments.

To Dario, Alessandro, Biagio and all my friends, for the support and advice they gave me.